8-Aryl-6-chloro-3-nitro-2-(phenylsulfonylmethyl)imidazo[1,2-a]pyridines as potent antitrypanosomatid molecules bioactivated by type 1 nitroreductases

Cyril Fersing, Clotilde Boudot, Julien Pedron, Sébastien Hutter, Nicolas Primas, Caroline Castera-Ducros, Sandra Bourgeade-Delmas, Moreau Alain, Anita D Cohen, Jean-Luc Stigliani, et al.

Published in final edited form as:
Eur J Med Chem. 2018 September 05; 157: 115–126. doi:10.1016/j.ejmech.2018.07.064.

8-Aryl-6-chloro-3-nitro-2-(phenylsulfonylmethyl)imidazo[1,2-*a*]pyridines as potent antitrypanosomatid molecules bioactivated by type 1 nitroreductases

Cyril Fersing[a,1], **Clotilde Boudot**[b,1], **Julien Pedron**[c], **Sébastien Hutter**[d], **Nicolas Primas**[a], **Caroline Castera-Ducros**[a], **Sandra Bourgeade-Delmas**[e], **Alix Sournia-Saquet**[c], **Alain Moreau**[c], **Anita Cohen**[d], **Jean-Luc Stigliani**[c], **Geneviève Pratviel**[c], **Maxime D. Crozet**[a], **Susan Wyllie**[f], **Alan Fairlamb**[f], **Alexis Valentin**[e], **Pascal Rathelot**[a], **Nadine Azas**[d], **Bertrand Courtioux**[b], **Pierre Verhaeghe**[c,*], **Patrice Vanelle**[a,**]

[a]Aix Marseille Univ, CNRS, ICR UMR 7273, Equipe Pharmaco-Chimie Radicalaire, FAC PHARM, 27 Boulevard Jean Moulin, CS30064, 13385, Marseille Cedex 05, France

[b]Université de Limoges, UMR Inserm 1094, Neuroépidémiologie Tropicale, Faculté de Pharmacie, 2 rue du Dr Marcland, 87025, Limoges, France

[c]LCC-CNRS Université de Toulouse, CNRS, UPS, Toulouse, France

[d]IHU Méditerranée Infection, Aix-Marseille Univ, UMR VITROME, 19-21 Boulevard Jean Moulin, 13005, Marseille, France

[e]UMR 152 PHARMA-DEV, Université de Toulouse, IRD, UPS, Toulouse, France

[f]University of Dundee, School of Life Sciences, Division of Biological Chemistry and Drug Discovery, Dow Street, Dundee, DD1 5EH, Scotland, United Kingdom

Abstract

Based on a previously identified antileishmanial 6,8-dibromo-3-nitroimidazo[1,2-*a*]pyridine derivative, a Suzuki-Miyaura coupling reaction at position 8 of the scaffold was studied and optimized from a 8-bromo-6-chloro-3-nitroimidazo[1,2-*a*]pyridine substrate. Twenty-one original derivatives were prepared, screened *in vitro* for activity against *L. infantum* axenic amastigotes and *T. brucei brucei* trypomastigotes and evaluated for their cytotoxicity on the HepG2 human cell line. Thus, 7 antileishmanial hit compounds were identified, displaying IC_{50} values in the 1.1–3 μM range. Compounds **13** and **23**, the 2 most selective molecules (SI = >18 or >17) were additionally tested on both the promastigote and intramacrophage amastigote stages of *L. donovani*. The two molecules presented a good activity (IC_{50} = 1.2–1.3 μM) on the promastigote stage but only molecule **23**, bearing a 4-pyridinyl substituent at position 8, was active on the intracellular amastigote stage, with a good IC_{50} value (2.3 μM), slightly lower than the one of miltefosine (IC_{50} = 4.3 μM). The antiparasitic screening also revealed 8 antitrypanosomal hit compounds, including **14** and **20**, 2 very active (IC_{50} = 0.04–0.16 μM) and selective (SI = >313 to 550) molecules toward *T. brucei brucei*, in comparison with drug-candidate fexinidazole (IC_{50} =

*Corresponding author. pierre.verhaeghe@univ-tlse3.fr (P. Verhaeghe). **Corresponding author. patrice.vanelle@univ-amu.fr (P. Vanelle).
[1]Co-first authors.

Europe PMC Funders Author Manuscripts

0.6 & SI > 333) or reference drugs suramin and eflornithine (respective IC_{50} = 0.03 and 13.3 μM). Introducing an aryl moiety at position 8 of the scaffold quite significantly increased the antitrypanosomal activity of the pharmacophore. Antikinetoplastid molecules **13**, **14**, **20** and **23** were assessed for bioactivation by parasitic nitroreductases (either in *L. donovani* or in *T. brucei brucei*), using genetically modified parasite strains that over-express NTRs: all these molecules are substrates of type 1 nitroreductases (NTR1), such as those that are responsible for the bioactivation of fexinidazole. Reduction potentials measured for these 4 hit compounds were higher than that of fexinidazole (−0.83 V), ranging from −0.70 to −0.64 V.

Keywords

Imidazo[1,2-*a*]pyridine; Nitroheterocycles; Suzuki-Miyaura cross-coupling reaction; Nitroreductases; *Leishmania*; *Trypanosoma*; *In vitro* activity; HepG2 cytotoxicity; SARs; Redox potentials

1 Introduction

Trypanosomatids are a group of kinetoplastid parasites infecting mammalians. Among trypanosomatids, *Leishmania* and *Trypanosoma* are the two main genera responsible for human infections that mainly occur in the intertropical region. Although these parasitic infections are lethal if untreated, there are very few efficacious, safe and affordable drugs available for treating infected patients with low income, living in developing countries. For this reason, the WHO classified trypanosomatid parasites among the infectious agents causing “neglected tropical diseases” [1,2].

The *Leishmania* parasites, mainly *L. donovani* and *L. infantum*, are responsible for leishmaniasis. Visceral leishmaniasis (VL) is the most severe clinical form with about 300.000 new cases and 20.000 annual deaths annually, according to the WHO [3]. Briefly, the parasite is transmitted by the bite of a *phlebotominae* sandfly, as a flagellated motile promastigote which disseminates into the organism and penetrates into macrophages where it transforms into an amastigote stage, resistant to phagocytosis and multiplies, causing organ and tissue damages, leading to death [4].

In the *Trypanosoma* genus, *T. brucei* (*gambiense* or *rhodesiense*) is one of the species responsible for human infections. It causes Human African Trypanosomiasis (HAT), also called sleeping sickness, affecting about 3.000 people annually, mainly in central Africa [5]. This parasitic disease occurs after the bite of a tsetse fly and develops in two clinical stages: a phase 1 peripheral haemolymphatic stage followed by a meningoencephalitic phase 2 in which the parasite crosses the blood-brain barrier and invades the central nervous system, leading to death [6].

There are very few therapeutic options for treating VL in endemic areas: Antimony V derivatives are facing high resistance levels and are toxic molecules, pentamidine is also quite toxic and must be administered IV, amphotericin B is very active but also highly nephrotoxic, must be administered IV and is very expensive as a liposomal formulation and miltefosine, the only orally available drug, is teratogenic [7]. The available treatments

Europe PMC Funders Author Manuscripts

against HAT carry similar disadvantages: pentamidine, melarsoprol, an arsenic derivative that is highly toxic, suramin which is only active on the phase 1 of the disease, and the eflornithine/nifurtimox combination for treating phase 2 [8,9].

Looking at the molecules studied as antileishmanial drug candidates [9,10], it must be noted that there is currently no novel chemical entity undergoing clinical trial against VL, at any stage [11], which is quite worrying. Regarding the antitrypanosomal pipeline, only acoziborole, a bore-containing molecule [9,11] and fexinidazole, a nitroaromatic compound [9,11,12], are new chemical entities in clinical development. At a pre-clinical stage of development, delamanid (a marketed antituberculosis treatment) is another nitroaromatic molecule displaying promising potential as an oral antileishmanial agent [13]. Thus, after several decades of abandonment, nitroaromatic derivatives are re-emerging as key molecules to fight against critical infectious diseases, displaying original mechanisms of action. As an antitrypanosomatid molecule, fexinidazole was first studied as an antileishmanial candidate [14]. It is a 5-nitroimidazole prodrug including a thioether group that is oxidized into an active sulfone metabolite (Fig. 1). Fexinidazole did not show sufficient clinical efficacy when used orally as a single therapy for the treatment of VL in a phase 2 clinical trial. Nevertheless, fexinidazole demonstrated good efficacy in pre-clinical studies against both peripheral [15] and central [16] stages of HAT and has recently completed a phase 3 clinical trial against HAT [12].

The antitrypanosomatid mechanism of action of fexinidazole depends on its bioactivation by parasite enzymes called nitroreductases (NTRs). Including a flavin co-factor, these enzymes catalyze the 1- or 2-electron reduction of nitroaromatic derivatives into electrophilic nitroso and hydroxylamine metabolites that are cytotoxic, forming covalent adducts with nucleophilic entities such as cysteine residues or DNA bases [17]. Interestingly, mammalian cells do not possess NTRs, allowing very good antiparasitic selectivity for nitroaromatic compounds. In *Leishmania*, two nitroreductases have been characterized: an essential type 1 mitochondrial NTR1, catalyzing the 2-electron reduction of nitroaromatics [18,19] and, recently, a type 2 NTR2, catalyzing the 1-electron reduction of nitroaromatics [20]. In *Trypanosoma*, only one NTR1 was characterized [21]. Unfortunately, apart from their primary sequence, there is no structural data available for any of these parasitic NTRs. They have never been crystallized nor co-crystallized, which limits the rational medicinal chemistry approaches to the design of novel substrates of NTRs, as antitrypanosomatid candidates.

The imidazo[1,2-*a*]pyridine ring is a well-known scaffold in pharmaceutical chemistry that has been extensively studied since the discovery of the hypnotic drug zolpidem (Ambien®, Stilnox®). Some imidazo[1,2-*a*]pyridine derivatives were reported as *in vitro* antileishmanial molecules [22] and our group previously reported the synthesis and biological evaluation of 3-nitroimidazo[1,2-*a*]pyridines, active on both promastigote and intramacrophage amastigote stages of *L. donovani* [23]. Thus, a hit compound was identified (Fig. 2), bearing 2 bromine atoms at positions 6 and 8, a nitro group at position 3 and a phenylsulfonylmethyl substituent at position 2 of the imidazo[1,2-*a*]pyridine ring. In this work, the nitro group appeared to be necessary for providing activity and the introduction of a bromine atom at position 8 of the scaffold appeared to increase antileishmanial activity [23].

From these encouraging preliminary results and based on a strategy that we previously applied to the antileishmanial pharmacomodulation of bicyclic nitroaromatic molecules using the Suzuki-Miyaura reaction [24], we decided to study the effect of introducing aryl moieties at position 8 of the 3-nitroimidazo[1,2-*a*]pyridine scaffold. Moreover, the new synthesized derivatives were not only studied for their antileishmanial activity, as done for the initial hit molecule, but also regarding their antitrypanosomal activity, to get a broader idea of the antiparasitic potential of the corresponding pharmacophore.

2 Results and discussion

Suzuki-Miyaura cross-coupling reactions at position 8 of the imidazo[1,2-*a*]pyridine ring were already reported [25]. However, when this ring is substituted by two bromine atoms at positions 6 and 8, the Suzuki-Miyaura coupling takes place at both positions [26]. To avoid this double coupling reaction and favor the selective functionalization at position 8 while maintaining a halogen atom at position 6 (to preserve the antiparasitic pharmacophore), a new substrate was prepared (Scheme 1). Adopting a previously reported synthesis strategy [27,28], 2-amino-5-chloropyridine was reacted with *N*-bromosuccinimide to afford 2-amino-3-bromo-5-chloropyridine **1** which was cyclized into the corresponding imidazo[1,2-*a*]pyridine derivative **2** by reaction with 1,3-dichloroacetone. The nitration of molecule **2**, in classical conditions, led to compound **3** which was engaged into a S_N2 reaction with the sodium salt of benzenesulfinic acid to form molecule **4**. Thus, an original substrate was prepared to conduct an antiparasitic pharmacomodulation study at position 8 *via* palladium-catalyzed coupling reactions.

Next, the Suzuki-Miyaura coupling reaction between **4** and phenylboronic acid was studied by varying several parameters such as nature and amount of catalyst, nature and amount of base, nature of solvent, reaction temperature and time, seeking an efficient operating procedure (Table 1). The initial conditions were inspired from a previously reported protocol involving 1.3 equiv. of phenylboronic acid, 10 mol% $Pd(PPh_3)_4$ and 3 equiv. of Na_2CO_3 in sealed tubes, under microwave (MW) heating [29]. The first studied parameter was the nature of the solvent (entries 1-10). By testing dioxane and dimethoxyethane (DME), it was rapidly noted that the total conversion of the substrate required to engage 5 equiv. of Na_2CO_3 (entries 3 and 4). Neither tetrahydrofuran (THF) nor water (or water/organic solvent mixtures) led to the same reaction yield as DME (49%, entry 4). Then, several bases were studied (entries 11-16) and the best result was obtained with K_2CO_3 (64%, entry 16). The use of three other Pd-containing catalysts (entries 17-19) did not show any improvement in reaction yield. When comparing entry 16 (best result) to conventional heating (entry 20) or to microwave heating at 95 °C (entry 21), it appeared that, with DME, the use of MW was favourable but increasing the reaction temperature was not. Finally, DME was replaced by THF and a very efficient procedure (90% yield) was achieved by heating at 120 °C in a sealed tube under MW for only 1 h (entry 25). In these efficient conditions, decreasing the amount of catalyst to 0.05 equiv. led to a poor reaction yield (36%, entry 26). To validate the operating conditions determined with phenylboronic acid, 2 other phenylboronic acid derivatives were engaged in the same reaction (entries 27-28), leading to comparable yields (84 and 87%) after 2 h.

As presented in Scheme 2, after optimizing the operating procedure, the reaction was extended to 20 other aryl- or heteroarylboronic acids, to synthesize a small library of novel derivatives bearing various aryl groups (substituted phenyl, thiophene, furan or pyridine) at position 8 of the imidazopyridine scaffold. The reaction yields varied from 90% (phenylboronic acid) to 41% (2-CF_3-phenylboronic acid) and were generally lower when using pyridinylboronic (51–53%) or furanylboronic (53%) acids. The X-ray structures of substrate **4** and coupling product **23** are presented in Fig. 3.

All synthesized compounds were tested *in vitro* for their cytotoxicity on the HepG2 human cell line and compared to a cytotoxic reference drug: doxorubicin (Table 2). Out of the 21 tested compounds, 8 molecules (**6**, **7**, **9**, **17**, **18**, **19**, **24** and **25**) could not be evaluated properly because of a lack of solubility in the culture medium. Thus, in comparison with the initial 8-brominated hit-compound (cLogP = 3.4), solubility in the culture medium was improved only when introducing a 4-pyridinyl or a 2-(hydroxymethyl)phenyl substituent at position 8 of the scaffold. Regarding the link between solubility in the aqueous culture medium and cLogP values in the studied series, it can be noted that all poorly soluble compounds (apart **25**) were the ones displaying cLogP values between 3.9 and 5.0 whereas the 2 most soluble compounds (**14** and **23**) were the ones displaying cLogP values of 3.4 and 2.9, respectively. Compound **12** was the most cytotoxic (CC_{50} = 13 μM), whereas compound **14** was the least cytotoxic (CC_{50} = 88 μM). Then, 13 molecules were screened *in vitro* for their activity against *L. infantum* axenic amastigotes and compared to 3 reference drugs (or drug candidate): amphotericin B, miltefosine and fexinidazole (Table 2). Seven molecules (**5**, **13**, **15**, **20**, **21**, **22**, **23**) appeared as new antileishmanial hit compounds by displaying good IC_{50} values (1.1–3 μM), close to the ones of miltefosine (0.8 μM) and fexinidazole (3.4 μM), together with selectivity index values above 10. Regarding antitrypanosomal activity, molecules were screened on the trypomastigote stage of *T. brucei brucei* and compared to 3 antitrypanosomal drugs (or drug candidate): eflornithine, suramin and fexinidazole (Table 2). Eight molecules (**10**, **12**, **13**, **14**, **20**, **21**, **22**, **23**) were considered as good antitrypanosomal hit compounds, presenting low IC_{50} values (0.04–0.25 μM), in comparison with all reference drugs, associated to high selectivity index values, ranging from >136 to 550. With respect to the initial hit compound (IC_{50} = 2.9 μM), it is important to note that introducing a phenyl or a pyridinyl group at position 8 of the pharmacophore strongly increased the antitrypanosomal activity. By combining all parameters, 5 molecules bearing a 3-(hydroxymethyl)phenyl (**13**), a CF_3-substituted phenyl (**20**, **21**) or pyridinyl (**22**, **23**) moiety at position 8 of the imidazo[1,2-*a*]pyridine ring, were the ones displaying a global antikinetoplastid profile.

To deeper evaluate the antileishmanial potential of molecules **13** and **23** (molecules with suitable aqueous solubility, low cytotoxicity, good activity and highest selectivity indices), an *in vitro* evaluation toward both the promastigote and the intramacrophage amastigote stage of *L. donovani* was carried out, after evaluating their cytotoxicity on the THP1 macrophage cell line (Table 3). The results showed that molecule **13**, containing a 3-(hydroxymethyl) phenyl moiety, was active on the promastigote stage but was not on the intramacrophage amastigote one whereas molecule **23**, presenting a 4-pyridinyl moiety, was active on both stages. Considering the key activity toward the intramacrophage amastigote

stage, molecule **23** was not only more active (IC_{50} = 2.3 μM) than the initial hit compound (IC_{50} = 5.5 μM), but was also slightly more active and selective (SI > 22) than miltefosine (IC_{50} = 4.3 μM, SI = 20) and as selective as amphotericin B (SI = 22). Neverthless, the aqueous solubility of hit molecule **23** remains to improve. Fexinidazole was not active *in vitro* toward the intramacrophage amastigote stage of *L. donovani*; only its sulfone metabolite is able to display intracellular activity [14–16].

To investigate the antiparasitic mechanism of action of these new nitrated molecules, we hypothesized that they could be substrates of kinetoplastid nitroreductases. This hypothesis was tested by comparing the IC_{50} values measured on wild-type parasite strains with the ones measured on recombinant parasite strains overexpressing a nitroreductase (Table 4). Thus, the activities of molecules **13** and **23** were determined in parallel on a *L. donovani* wild-type strain (promastigote stage) and on two *L. donovani* strains overexpressing either NTR1 [19] or NTR2 [20]. As noted with the initial hit molecule, compounds **13** and **23** are selectively bioactivated by *L. donovani* NTR1 as their IC_{50} values are 20–40 times lower on the NTR1 overexpressing strain than on the wild type one. The same approach was followed with compounds **14** and **20**. Their activities toward a wild type strain of *T. brucei brucei* (trypomastigote stage) and a recombinant strain overexpressing NTR1 [21] were compared (Table 4). Like with nifurtimox, used as a reference drug, the tested molecules were more active (two-fold increase in activity) on the strain overexpressing NTR1. Interestingly, these molecules, especially compound **20**, were much more active than nifurtimox toward *T. brucei brucei*. It can then be concluded that molecules **13, 14, 20** and **23** are novel antikinetoplastid nitroaromatic compounds that are bioactivated by type 1 nitroreductases (NTR1), the same enzymes as the ones involved in the mechanism of action of fexinidazole by generating cytotoxic reduction metabolites [14].

Finally, an electrochemical study was done by measuring the reduction potentials of 7 molecules belonging to the studied series, using cyclic voltammetry, and comparing them to the one of fexinidazole (Table 5). For all tested molecules, a reversible single electron reduction was observed, corresponding to the formation of a nitro radical anion (see supplementary data). The redox potentials of all molecules belonging to the 3-nitroimidazo[1,2-*a*]pyridine series ranged from −0.7 to −0.6 V and were higher than that of fexinidazole (E° = −0.83 V). When comparing brominated molecule **4** to the Suzuki-Miyaura coupling product **5**, bearing a phenyl moiety, it can be noted that the phenyl ring slightly reduces the E° value (−0.69 *versus* −0.65 V). Introducing electron-donating (–CH_2OH) or electron-withdrawing (–CF_3) groups on the phenyl ring at position 2 or 3 has a very limited influence on the redox potential (±0.01 or 0.02 V), whereas substituting a 4-pyridinyl moiety to the phenyl ring slightly increases the redox potential (−0.64 *versus* −0.69 V). Comparison of molecule **4** (8-bromo-6-chloro) to the initial hit (6,8-dibromo), showed that substituting a chlorine atom for a bromine atom at position 6 of the imidazo[1,2-*a*]pyridine ring decreases the E° value from −0.59 to −0.65 V. These results indicate that, in the studied series, it is possible to improve the antikinetoplastid activity while significantly decreasing the redox potential values from −0.59 V (initial hit) to −0.70 V (**13** and **14**), this last value remaining compatible with kinetoplastid NTR1 enzymatic capabilities. Starting from the initial hit compound, this decrease in E° value was achieved by introducing a

chlorine atom at position 6 of the 3-nitroimidazo[1,2-*a*]pyridine scaffold and by introducing a phenyl group at position 8.

Katsuno and co-workers [30] proposed a list of criteria to define antileishmanial and antitrypanosomal hit compounds, including original structure, easy synthesis (up to 5 reaction steps), IC_{50} < 10 μM (both on the promastigote and intramacrophage amastigote stages for *Leishmania*) and selectivity index > 10 (in comparison with mammalian cells). Of the 21 tested molecules, compound **23** meets all these criteria for an antileishmanial molecule and 13 compounds meet the same criteria for antitrypanosomal molecules.

3 Conclusion

To design novel antitrypanosomatid molecules, a selective Suzuki-Miyaura coupling reaction was developed at position 8 of a 6,8-dihalogeno-3-nitroimidazo[1,2-*a*]pyridine antileishmanial pharmacophore which was previously identified. A series of 21 new derivatives was prepared and screened *in vitro* toward *Leishmania* and *Trypanosoma*, highlighting 1 antileishmanial (molecule **23**) and several antitrypanosomal (including **14** and **20**) hit compounds with high activities (0.04 μM < IC_{50} < 3 μM) and good to excellent selectivity (10 < SI < 550) *versus* the HepG2 human cell line. Replacing the bromine atom at position 8 by aryl moieties particularly improved the antitrypanosomal activity. All derivatives appeared to be metabolized by type 1 nitroreductases (NTR1) in both *Leishmania* and *Trypanosoma*; their mechanism of action is therefore probably analogous to that of drug candidate fexinidazole. Indeed, the redox potentials of these new hit compounds were lower than that of the previously identified and less active hit molecule (−0.59 V), ranging from −0.7 to −0.6 V. Although a slight improvement in the aqueous solubility of this promising chemical series was achieved by introducing a 4-pyridinyl moiety, water solubility remains to be improved in order to achieve optimal properties for initiating *in vivo* studies on mouse models.

3.1 Experimental section

3.1.1 Chemistry

3.1.1.1 General procedures: All commercially available solvents and reagents were purchased from commercial suppliers (Fluorochem or Sigma Aldrich) and used without further purification. Melting points were determined in open capillary tubes with a Büchi apparatus and are uncorrected. ^{1}H and ^{13}C NMR spectra were determined on a Brucker Avance 200, 300 or 400 MHz instrument at the Faculté de Pharmacie de Marseille, Faculté des Sciences de St Jérôme (Marseille) and at the Laboratoire de Chimie de Coordination of Toulouse. Chemical shifts are given in δ values referenced to the solvent and using tetramethylsilane (TMS) as an internal standard. High resolution mass spectra were recorded on a QStar Elite mass spectrometer at the Spectropôle department of the Faculté des Sciences de St Jérôme. Silica Gel 60 (Merk 70–230) was used for column chromatography. TLC was performed on aluminium plates coated with silica gel 60F-254 (Merk) in an appropriate eluent. Visualisation was made with ultraviolet light (234 nm). Progress of the reactions and purity of the synthesized compounds were checked with LC-MS analyses which were realized at the Faculté de Pharmacie de Marseille on a Thermo Scientific Accela

High Speed LC System® coupled with a single quadrupole mass spectrometer Thermo MSQ Plus®. The RP-HPLC column used is a Thermo Hypersil Gold® 50 × 2.1 mm (C13 bounded), with particles of 1.9 μM diameter. The volume of sample injected on the column was 1 μL. The chromatographic analysis, total duration of 8 min, is made with the following gradient of solvents: t = 0 min, water/methanol 50/50; 0 < t < 4 min, linear increase in the proportion of water to a water/methanol ratio of 95/5; 4 < t < 6 min, water/methanol 95/5; 6 < t < 7 min, linear decrease in the proportion of water to return to a ratio water/methanol of 50/50; 6 < t < 7 min, water/methanol 50/50. The water used was buffered with 5 mM ammonium acetate. The microwave reactions were performed in sealed vials, using a Biotage Initiator or CEM Discover SP-D microwave oven.

3.1.1.2 Synthesis: 3-Bromo-5-chloropyridin-2-amine (1) [31]: To a solution of 5-chloropyridin-2-amine (10 g, 77.8 mmol, 1 equiv.) in acetonitrile (150 mL), *N*-bromosuccinimide (13.8 g, 77.8 mmol, 1 equiv.) was added. The reaction mixture was stirred and refluxed for 1 h. Then the solvent was evaporated *in vacuo*. Compound **1** was obtained, after purification by chromatography on silica gel (eluent: dichloromethane–ethyl acetate 9:1) and recrystallization from propan-2-ol as a pale beige solid in 71% yield. mp: 82 °C, Lit.: 83–84 °C; ^{1}H NMR (400 MHz, [D_6]DMSO) *δ*: 6.43 (2H, s), 7.88 (1H, d, *J* = 2.2 Hz), 7.96 (1H, d, *J* = 2.2 Hz), ^{13}C NMR (100 MHz, [D_6]DMSO) *δ*: 103.0 (C), 117.1 (C), 139.0 (CH), 145.0 (CH), 155.3 (C); MS ESI^{+} (*m*/*z*): 207.27/209.32 [M+H]$^{+}$.

8-Bromo-6-chloro-2-chloromethylimidazo[1,2-*a*]pyridine (2): To a solution of 3-bromo-5-chloropyridin-2-amine **1** (10 g, 48.2 mmol, 1 equiv.) in ethanol (150 mL), 1,3-dichloroacetone (6.68 g, 53 mmol, 1.1 equiv.) was added. The reaction mixture was stirred and heated under reflux for 96 h. The solvent was then evaporated *in vacuo*. Compound **2** was obtained, after purification by chromatography on silica gel (eluent: dichloromethane–ethyl acetate 9:1) and recrystallization from diethyl ether as a white solid in 60% yield. mp: 161 °C; ^{1}H NMR (400 MHz, $CDCl_3$) *δ*: 4.78 (2H, s), 7.47 (1H, d, *J* = 1.7 Hz), 7.70 (1H, br s), 8.12 (1H, d, *J* = 1.7 Hz); ^{13}C NMR (100 MHz, $CDCl_3$) *δ*: 39.3 (CH_2), 111.9 (C), 113.2 (CH), 120.5 (C), 123.1 (CH), 128.7 (CH), 141.9 (C), 145.1 (C); MS ESI^{+} (*m*/*z*): 280.99/282.97 [M+H]$^{+}$; HRMS (+ESI): 280.9064 [M + H]$^{+}$; Calcd for $C_8H_5N_2BrCl_2$: 280.9062.

8-Bromo-6-chloro-2-chloromethyl-3-nitroimidazo[1,2-*a*]pyridine (3): To a solution of 8-bromo-6-chloro-2-chloromethylimidazo[1,2-*a*]pyridine **2** (5 g, 18 mmol, 1 equiv.) in concentrated sulfuric acid (50 mL) cooled by an ice-water bath, nitric acid 65% (5 mL, 0.11 mol, 6 equiv.) was added. The reaction mixture was stirred for 1 h at room temperature. Then, the mixture was slowly poured into an ice-water mixture and the desired product precipitated. The yellow solid was collected by filtration, dried under reduced pressure and recrystallized from propan-2-ol to give the expected product **3** in 60% yield. mp 165 °C; ^{1}H NMR (400 MHz, $CDCl_3$) *δ*: 5.09 (2H, s), 7.92 (1H, d, *J* = 1.8 Hz), 9.49 (1H, d, J = 1.8 Hz); ^{13}C NMR (100 MHz, $CDCl_3$) *δ*: 38.3 (CH_2), 113.3 (C), 124.8 (CH), 125.3 (C), 129.9 (C), 134.2 (CH), 141.0 (C), 147.7 (C); MS ESI^{+} (*m*/*z*): 324.00/325.93 [M+H]$^{+}$; HRMS (+ESI): 323.8938 [M + H]$^{+}$; Calcd for $C_8H_4N_3O_2BrCl_2$: 323.8937.

8-Bromo-6-chloro-3-nitro-2-(phenylsulfonylmethyl)imidazo[1,2-*a*]pyridine (4): To a solution of 8-bromo-6-chloro-2-chloromethyl-3-nitroimidazo[1,2-*a*]pyridine **3** (5 g, 15.39 mmol, 1 equiv.) in dimethylsulfoxide (150 mL), sodium benzenesulfinate (7.58 g, 46.17 mmol, 3 equiv.) was added. The reaction mixture was stirred for 3 h at room temperature. The reaction mixture was then slowly poured into an ice-water mixture, making the desired product precipitate. The pale orange solid was collected by filtration, dried under reduced pressure and recrystallized from acetonitrile to give the expected product **4** in 80% yield. mp 196 °C; ^{1}H NMR (400 MHz, $CDCl_3$) δ: 5.14 (2H, s), 7.52–7.56 (2H, m), 7.66–7.69 (1H, m), 7.84–7.89 (3H, m), 9.42 (1H, br s); ^{13}C NMR (100 MHz, $CDCl_3$) δ: 56.8 (CH_2), 113.3 (C), 124.8 (CH), 125.4 (C), 128.6 (2CH), 129.4 (2CH), 131.8 (C), 134.2 (CH), 134.4 (CH), 139.2 (C), 139.8 (C), 141.1 (C); MS ESI$^+$ (*m*/*z*): 429.84/431.82 $[M+H]^+$. HRMS (+ESI): 431.9236 $[M + H]^+$; Calcd for $C_{14}H_9N_3O_4SClBr$: 431.9236.

General procedure for the preparation of 8-arylimidazo[1,2-*a*]pyridine derivatives (5 to 25): A mixture of 8-bromo-6-chloro-3-nitro-2-(phenylsulfonylmethyl)imidazo[1,2-*a*]pyridine (400 mg, 1 equiv.), tetrakis(triphenylphosphine)palladium(0) (0.1 equiv., 107.3 mg), potassium carbonate (5 equiv., 642 mg), and appropriate boronic acid (1.3 equiv.) in THF (15 mL) under N_2 atmosphere was heated at 120 °C under microwave irradiation until complete disappearance of the starting material (as monitored by LC/MS or TLC). Water was then added and the mixture was extracted three times with dichloromethane. The organic layer was washed three times with water, dried over $MgSO_4$, filtered and evaporated. The crude residue was purified by column chromatography on silica gel and recrystallized from the appropriate solvent, affording compounds **5** to **25**.

6-Chloro-3-nitro-8-phenyl-2-(phenylsulfonylmethyl)imidazo[1,2-*a*]pyridine (5): Compound **5** was obtained after purification by chromatography (eluent: dichloromethane/cyclohexane/diethyl ether 6.5/3/0.5) and recrystallization from acetonitrile as a yellow solid in 90% yield (0.36 g). mp 201 °C. ^{1}H NMR (400 MHz, $CDCl_3$) δ: 5.18 (s, 2H), 7.45–7.49 (m, 3H), 7.52–7.56 (m, 2H), 7.68–7.72 (m, 4H), 7.87–7.89 (m, 2H), 9.47 (d, J = 1.9 Hz, 1H). ^{13}C NMR (100 MHz, $CDCl_3$) δ: 56.7 (CH_2), 124.3 (CH), 126.2 (C), 128.7 (2CH), 129.0 (2CH), 129.4 (2CH), 129.5 (2CH), 130.0 (CH), 130.4 (CH), 131.2 (C), 132.0 (C), 133.1 (C), 134.1 (CH), 139.4 (C), 139.7 (C), 141.9 (C). MS ESI$^+$ (*m*/*z*): 427.98/429.87 $[M+H]^+$. HRMS (+ESI): 428.0464 $[M + H]^+$. Calcd for $C_{20}H_{14}N_3O_4SCl$: 428.0466.

6-Chloro-8-(4-chlorophenyl)-3-nitro-2-(phenylsulfonylmethyl)imidazo[1,2-*a*]pyridine (6): Compound **6** was obtained after purification by chromatography (eluent: dichloromethane/cyclohexane/diethyl ether 6.5/3/0.5) as a pale yellow solid in 74% yield (0.32 g). mp 250 °C; ^{1}H NMR (400 MHz, $[D_6]$DMSO) δ: 5.29 (s, 2H), 7.48–7.50 (m, 2H), 7.62–7.69 (m, 4H), 7.80–7.87 (m, 3H), 8.13 (d, J = 1.7 Hz, 1H), 9.37 (d, J = 1.7 Hz, 1H); ^{13}C NMR (100 MHz, $[D_6]$DMSO) δ: 55.6 (CH_2), 124.4 (C), 125.1 (CH), 128.3 (2CH), 128.4 (2CH), 128.8 (C), 129.4 (2CH), 130.4 (CH), 131.2 (2CH), 131.7 (C), 132.6 (C), 134.2 (CH), 134.4 (C), 138.6 (C), 139.4 (C), 140.9 (C); MS ESI$^+$ (*m*/*z*): 461.89/463.84 $[M+H]^+$; HRMS (+ESI): 462.0074 $[M + H]^+$; Calcd for $C_{20}H_{13}N_3O_4SCl_2$: 462.0077.

6-Chloro-8-(4-methoxyphenyl)-3-nitro-2-(phenylsulfonylmethyl)imidazo[1,2-*a*]pyridine (7): Compound **7** was obtained after purification by chromatography (eluent:

dichloromethane/cyclohexane/diethyl ether 5.5/4/0.5) and recrystallization from acetonitrile as a yellow solid in 84% yield (0.36 g). mp 246 °C; ^{1}H NMR (400 MHz, [D$_6$]DMSO) δ: 3.85 (s, 3H), 5.30 (s, 2H), 6.97 (d, J = 8.9 Hz, 2H), 7.63–7.69 (m, 4H), 7.82–7.86 (m, 3H), 8.4 (d, J = 1.9 Hz, 1H), 9.31 (d, J = 1.9 Hz, 1H); ^{13}C NMR (100 MHz, [D$_6$] DMSO) δ: 55.3 (CH_3), 55.6 (CH_2), 113.8 (2CH), 123.9 (CH), 124.5 (C), 125.0 (C), 128.3 (2CH), 129.2 (CH), 129.3 (2CH), 129.8 (C), 130.8 (2CH), 131.0 (C), 134.1 (CH), 138.7 (C), 139.2 (C), 141.1 (C), 160.2 (C); MS ESI$^+$ (m/z): 457.94/459.96 [M+H]$^+$; HRMS (+ESI): 458.0569 [M + H]$^+$; Calcd for $C_{21}H_{16}N_3O_5SCl$: 458.0572.

4-(6-Chloro-3-nitro-2-(phenylsulfonylmethyl)imidazo[1,2-*a*]pyridin-8-yl)-N,N-diethylaniline (8): Compound **8** was obtained after purification by chromatography (eluent: dichloromethane/cyclohexane/diethyl ether 4.5/5/0.5) and recrystallization from acetonitrile as a red solid in 50% yield (0.23 g). mp 188 °C; ^{1}H NMR (400 MHz, [D$_6$]DMSO) δ: 1.14 (t, J = 6 Hz, 6H), 3.40–3.44 (m, 4H), 5.30 (s, 2H), 6.62 (d, J = 8.2 Hz, 2H), 7.61–7.68 (m, 4H), 7.80–7.94 (m, 4H), 9.20 (s, 1H); ^{13}C NMR (100 MHz, [D$_6$]DMSO) δ: 12.5 ($2CH_3$), 43.7 ($2CH_2$), 55.7 (CH_2), 110.8 (2CH), 118.5 (C), 122.4 (CH), 124.7 (C), 127.2 (CH), 128.3 (2CH), 129.4 (2CH), 130.4 (C), 130.5 (2CH), 130.8 (C), 134.0 (CH), 138.8 (C), 138.9 (C), 141.1 (C), 148.1 (C); MS ESI$^+$ (m/z): 498.81/500.87 [M+H]$^+$; HRMS (+ESI): 499.1204 [M + H]$^+$; Calcd for $C_{24}H_23N_4O_4SCl$: 499.1201.

4-(6-Chloro-3-nitro-2-(phenylsulfonylmethyl)imidazo[1,2-*a*]pyridin-8-yl)benzonitrile (9): Compound **9** was obtained after purification by chromatography (eluent: dichloromethane/cyclohexane/diethyl ether 5.5/3.5/1) and recrystallization from acetonitrile as a beige solid in 65% yield (0.27 g). mp 258 °C; ^{1}H NMR (400 MHz, [D$_6$]DMSO) δ: 5.30 (s, 2H), 7.63–7.67 (m, 2H), 7.81–7.86 (m, 4H), 7.88–7.92 (m, 3H), 8.22 (s, 1H), 9.42 (s, 1H); ^{13}C NMR (100 MHz, [D$_6$]DMSO) δ: 55.5 (CH_2), 111.9 (C), 118.5 (C), 124.3 (C), 125.8 (CH), 128.1 (C), 128.4 (2CH), 129.3 (2CH), 130.2 (2CH), 131.2 (CH), 131.8 (C), 132.1 (2CH), 134.2 (CH), 137.4 (C), 138.5 (C), 139.4 (C), 140.8 (C); MS ESI$^+$ (m/z): 452.84/4754.94 [M+H]$^+$. HRMS (+ESI): 453.0418 [M + H]$^+$; Calcd for $C_{21}H_{13}N_4O_4SCl$: 453.0419.

4-(6-Chloro-3-nitro-2-(phenylsulfonylmethyl)imidazo[1,2-*a*]pyridin-8-yl)benzaldehyde (10): Compound 10 was obtained after purification by chromatography (eluent: dichloromethane/cyclohexane/diethyl ether 5/4/1) and recrystallization from acetonitrile as a yellow solid in 62% yield (0.26 g). mp 221 °C; ^{1}H NMR (400 MHz, [D$_6$]DMSO) δ: 5.31 (s, 2H), 7.64–7.67 (m, 2H), 7.82–7.87 (m, 5H), 7.93–7.95 (m, 2H), 8.22 (d, J = 1.8 Hz, 1H), 9.41 (d, J = 1.8 Hz, 1H), 10.10 (s, 1H); ^{13}C NMR (100 MHz, [D$_6$]DMSO) δ: 55.6 (CH_2), 124.3 (C), 125.6 (CH), 128.4 (2CH), 128.8 (C), 129.2 (2CH), 129.3 (2CH), 130.1 (2CH), 131.0 (CH), 131.1 (C), 134.1 (CH), 136.2 (C), 138.4 (C), 138.6 (C), 139.4 (C), 140.9 (C), 192.8 (C); MS ESI$^+$ (m/z): 455.95/458.01 [M+H]$^+$; HRMS (+ESI): 456.0417 [M + H]$^+$; Calcd for $C_{21}H_{14}N_3O_5SCl$: 456.0415.

4-(6-Chloro-3-nitro-2-(phenylsulfonylmethyl)imidazo[1,2-*a*]pyridin-8-yl)phenol (11): Compound **11** was obtained after purification by chromatography (eluent: dichloromethane/cyclohexane/diethyl ether 5/3/2) and recrystallization from acetonitrile as a yellow solid in 66% yield (0.27 g). mp 267 °C; ^{1}H NMR (400 MHz, [D$_6$]DMSO) δ: 5.30 (s, 2H), 6.76–6.79

(m, 2H), 7.52–7.55 (m, 2H), 7.61–7.67 (m, 2H), 7.81–7.84 (m, 3H), 7.97 (d, *J* = 1.7 Hz, 1H), 9.28 (d, *J* = 1.7 Hz, 1H), 9.92 (s, 1H); ^{13}C NMR (100 MHz, [D_6] DMSO) *δ*: 55.6 (CH_2), 115.2 (2CH), 123.4 (C), 123.6 (CH), 124.6 (C), 128.4 (2CH), 128.8 (CH), 129.3 (2CH), 130.2 (C), 130.9 (2CH), 131.0 (C), 134.0 (CH), 138.7 (C), 139.15 (C), 141.1 (C), 158.8 (C); MS ESI$^+$ (*m*/*z*): 443.86/445.84 [M+H]$^+$; HRMS (+ESI): 444.0412 [M + H]$^+$; Calcd for $C_{20}H_{14}N_3O_5SCl$: 444.0415.

{4-[6-Chloro-3-nitro-2-(phenylsulfonylmethyl)imidazo[1,2-*a*]pyridin-8-yl]phenyl}methanol (12): Compound **12** was obtained after purification by chromatography (eluent: dichloromethane/cyclohexane/diethyl ether 4.5/4.5/1) and recrystallization from acetonitrile as a yellow solid in 54% yield (0.23 g). mp 244 °C; ^{1}H NMR (400 MHz, [D_6]DMSO) *δ*: 4.57 (s, 2H), 4.66 (bs, 1H), 5.30 (s, 2H), 7.33–7.37 (m, 2H), 7.59–7.67 (m, 4H), 7.81–7.85 (m, 3H), 8.08 (d, *J* = 1.9 Hz, 1H), 9.35 (d, *J* = 1.9 Hz, 1H); ^{13}C NMR (100 MHz, [D_6] DMSO) *δ*: 55.7 (CH_2), 62.5 (CH_2), 124.4 (C), 124.5 (CH), 126.3 (2CH), 128.4 (2CH), 129.2 (2CH), 129.3 (2CH), 129.9 (CH), 130.2 (C), 131.0 (C), 131.1 (C), 134.1 (CH), 138.7 (C), 139.3 (C), 141.2 (C), 144.0 (C); MS ESI$^+$ (*m*/*z*): 457.84/459.71 [M+H]$^+$; HRMS (+ESI): 458.0571 [M + H]$^+$; Calcd for $C_{21}H_{16}N_3O_5SCl$: 458.0572.

{3-[6-Chloro-3-nitro-2-(phenylsulfonylmethyl)imidazo[1,2-*a*]pyridin-8-yl]phenyl}methanol (13): Compound **13** was obtained after purification by chromatography (eluent: dichloromethane/cyclohexane/diethyl ether 6/2/2) and recrystallization from acetonitrile as a yellow solid in 52% yield (0.22 g). mp 210 °C; ^{1}H NMR (400 MHz, [D_6]DMSO) *δ*: 4.54 (d, *J* = 5.3 Hz, 2H), 5.29 (s, 3H), 7.34–7.50 (m, 3H), 7.60–7.66 (m, 3H), 7.79–7.82 (m, 3H), 8.06 (s, 1H), 9.37 (s, 1H); ^{13}C NMR (100 MHz, [D_6]DMSO) *δ*: 55.8 (CH_2), 62.7 (CH_2), 124.4 (C), 124.7 (CH), 127.1 (CH), 127.5 (CH), 128.0 (CH), 128.1 (CH), 128.3 (2CH), 129.3 (2CH), 130.2 (CH), 130.5 (C), 131.1 (C), 132.7 (C), 134.2 (CH), 138.7 (C), 139.4 (C), 141.2 (C), 143.0 (C); MS ESI$^+$ (*m*/*z*): 457.80/459.80 [M+H]$^+$; HRMS (+ESI): 458.0572 [M + H]$^+$; Calcd for $C_{21}H_{16}N_3O_5SCl$: 458.0572.

{2-[6-Chloro-3-nitro-2-(phenylsulfonylmethyl)imidazo[1,2-*a*]pyridin-8-yl]phenyl}methanol (14): Compound **14** was obtained after purification by chromatography (eluent: dichloromethane/cyclohexane/diethyl ether 8/1/1) and recrystallization from propan-2-ol as a yellow solid in 62% yield (0.26 g). mp 170 °C; ^{1}H NMR (400 MHz, [D_6]DMSO) *δ*: 4.31 (s, 2H), 5.03 (s, 1H), 5.22 (s, 2H), 7.18–7.20 (m, 1H), 7.31–7.36 (m, 1H), 7.45–7.50 (m, 1H), 7.54–7.59 (m, 3H), 7.72–7.75 (m, 3H), 7.91 (s, 1H), 9.39 (s, 1H); ^{13}C NMR (100 MHz, [D_6]DMSO) *δ*: 55.7 (CH_2), 60.9 (CH_2), 123.9 (C), 125.0 (CH), 126.5 (CH), 127.8 (CH), 128.1 (2CH), 128.8 (CH), 129.2 (2CH), 130.4 (CH), 130.8 (CH), 130.9 (C), 131.8 (C), 131.9 (C), 134.0 (CH), 138.7 (C), 139.4 (C), 140.7 (C), 141.7 (C); MS ESI$^+$ (*m*/*z*): 457.93/459.98 [M+H]$^+$; HRMS (+ESI): 458.0575 [M + H]$^+$; Calcd for $C_{21}H_{16}N_3O_5SCl$: 458.0572.

6-Chloro-8-(4-fluorophenyl)-3-nitro-2-(phenylsulfonylmethyl)imidazo[1,2-*a*]pyridine (15): Compound **15** was obtained after purification by chromatography (eluent: dichloromethane/cyclohexane/diethyl ether 5.5/4/0.5) and recrystallization from acetonitrile as a yellow solid in 64% yield (0.26 g). mp 211 °C; ^{1}H NMR (400 MHz, [D_6]DMSO) *δ*: 5.30 (s, 2H), 7.27 (t, *J* = 8.8 Hz, 2H), 7.63–7.72 (m, 4H), 7.81–7.87 (m, 3H), 8.09 (d, *J* = 1.8

Hz, 1H), 9.35 (d, *J* = 1.8 Hz, 1H); ^{13}C NMR (100 MHz, [D$_6$]DMSO) *δ*: 55.5 (CH_2), 115.3 (d, *J* = 21.6 Hz, 2CH), 124.4 (C), 124.7 (CH), 128.3 (2CH), 129.0 (C), 129.2 (d, *J* = 3.1 Hz, C), 129.3 (2CH), 130.2 (CH), 131.0 (C), 131.6 (d, *J* = 8.5 Hz, 2CH), 134.1 (CH), 138.6 (C), 139.3 (C), 141.0 (C), 162.7 (d, *J* = 247.7 Hz, C); MS ESI$^+$ (*m*/*z*): 445.81/447.12 [M+H]$^+$; HRMS (+ESI): 446.0372 [M + H]$^+$; Calcd for $C_{20}H_{13}N_3O_4SFCl$: 446.0372.

6-Chloro-8-(3-fluorophenyl)-3-nitro-2-(phenylsulfonylmethyl)imidazo[1,2-*a*]pyridine (16): Compound **16** was obtained after purification by chromatography (eluent: dichloromethane/cyclohexane/diethyl ether 6/3.5/0.5) and recrystallization from propan-2-ol as a yellow solid in 63% yield (0.26 g). mp 192 °C; ^{1}H NMR (400 MHz, [D$_6$]DMSO) *δ*: 5.30 (s, 2H), 7.31 (t, *J* = 8 Hz, 1H), 7.44–7.63 (m, 5H), 7.75–7.82 (m, 3H), 8.16 (s, 1H), 9.38 (s, 1H); ^{13}C NMR (100 MHz, [D$_6$]DMSO) *δ*: 55.6 (CH_2), 116.0 (d, *J* = 3.6 Hz, CH), 116.3 (C), 124.3 (C), 125.1 (CH), 125.5 (d, *J* = 2.8 Hz, CH), 128.2 (2CH), 128.6 (d, *J* = 2.4 Hz, C), 129.2 (2CH), 130.3 (d, *J* = 8.4 Hz, CH), 130.6 (CH), 131.1 (C), 134.1 (CH), 134.9 (d, *J* = 8.6 Hz, CH), 138.6 (C), 139.3 (C), 140.9 (C), 161.8 (d, *J* = 243.5 Hz, C); MS ESI$^+$ (*m*/*z*): 445.79/447.14 [M+H]$^+$; HRMS (+ESI): 446.0370 [M + H]$^+$; Calcd for $C_{20}H_{13}N_3O_4SFCl$: 446.0372.

6-Chloro-8-(2-fluorophenyl)-3-nitro-2-(phenylsulfonylmethyl)imidazo[1,2-*a*]pyridine (17): Compound **17** was obtained after purification by chromatography (eluent: dichloromethane/cyclohexane/diethyl ether 4.7/5/0.3) and recrystallization from propan-2-ol as a yellow solid in 71% yield (0.29 g). mp 220 °C; ^{1}H NMR (400 MHz, [D$_6$]DMSO) *δ*: 5.26 (s, 2H), 7.26–7.42 (m, 3H), 7.53–7.61 (m, 3H), 7.76–7.78 (m, 3H), 8.05 (s, 1H), 9.41 (s, 1H); ^{13}C NMR (100 MHz, [D$_6$]DMSO) *δ*: 55.7 (CH_2), 115.9 (d, *J* = 21.6 Hz, CH), 120.8 (d, *J* = 14 Hz, C), 123.8 (C), 124.3 (d, *J* = 3.5 Hz, CH), 125.3 (C), 125.6 (CH), 128.2 (2CH), 129.2 (2CH), 131.1 (C), 131.5 (d, *J* = 8.5 Hz, CH), 132.2 (d, *J* = 2.1 Hz, CH), 132.3 (d, *J* = 2.9 Hz, CH), 134.0 (CH), 138.7 (C), 139.5 (C), 141.2 (C), 159.2 (d, *J* = 248.5 Hz, C); MS ESI$^+$ (*m*/*z*): 445.88/447.14 [M+H]$^+$; HRMS (+ESI): 446.0369 [M + H]$^+$; Calcd for $C_{20}H_{13}N_3O_4SFCl$: 446.0372.

6-Chloro-8-(2,4-difluorophenyl)-3-nitro-2-(phenylsulfonylmethyl)imidazo[1,2-*a*]pyridine (18): Compound **18** was obtained after purification by chromatography (eluent: dichloromethane/cyclohexane/diethyl ether 4.5/5/0.5) and recrystallization from acetonitrile as a yellow solid in 61% yield (0.26 g). mp 232 °C; ^{1}H NMR (300 MHz, [D$_6$]DMSO) *δ*: 5.25 (s, 2H), 7.16–7.23 (td, *J* = 2.2 Hz and 8.5 Hz, 1H), 7.41–7.50 (m, 2H), 7.57–7.62 (m, 2H), 7.76–7.81 (m, 3H), 8.06 (s, 1H), 9.41 (d, *J* = 1.7 Hz, 1H); ^{13}C NMR (75 MHz, [D$_6$]DMSO) *δ*: 55.6 (CH_2), 104.4 (t, *J* = 26.5 Hz, CH), 111.5 (dd, *J* = 3.7 Hz and 21.4 Hz, CH), 117.4 (dd, *J* = 3.7 Hz and 14.3 Hz, C), 123.8 (C), 124.4 (C), 125.7 (CH), 128.2 (2CH), 129.2 (2CH), 131.1 (C), 132.3 (d, *J* = 3.3 Hz, CH), 133.4 (dd, *J* = 3.8 Hz and 10.2 Hz, CH), 134.0 (CH), 139.1 (d, *J* = 62.6 Hz, C), 141.1 (C), 157.9 (d, *J* = 12.8 Hz, C), 161.2 (d, *J* = 14.7 Hz, C), 164.5 (d, *J* = 12.5 Hz, C); MS ESI$^+$ (*m*/*z*): 463.85/465.80 [M+H]$^+$; HRMS (+ESI): 464.0280 [M + H]$^+$; Calcd for $C_{20}H_{12}N_3O_4SF2Cl$: 464.0278.

6-Chloro-3-nitro-2-(phenylsulfonylmethyl)-8-(4-trifluoromethylphenyl)imidazo[1,2-*a*]pyridine (19): Compound **19** was obtained after purification by chromatography (eluent: dichloromethane/cyclohexane/diethyl ether 5/4.5/0.5) and recrystallization from propan-2-ol

as a yellow solid in 87% yield (0.40 g). mp 231 °C; ^{1}H NMR (300 MHz, [D$_6$]DMSO) δ: 5.29 (s, 2H), 7.61–7.67 (m, 2H), 7.75–7.86 (m, 7H), 8.19 (d, J = 1.7 Hz, 1H), 9.40 (d, J = 1.7 Hz, 1H); ^{13}C NMR (75 MHz, [D$_6$]DMSO) δ: 55.6 (CH_2), 124.0 (q, J = 272.4 Hz, CF_3), 124.4 (C), 125.1 (q, J = 3.7 Hz, 2CH), 125.6 (CH), 128.4 (2CH), 128.6 (C), 129.3 (2CH), 129.5 (q, J = 32 Hz, C), 130.2 (2CH), 131.0 (CH), 131.1 (C), 134.1 (CH), 136.9 (C), 138.6 (C), 139.5 (C), 140.9 (C); MS ESI$^+$ (m/z): 495.80/497.91 [M+H]$^+$; HRMS (+ESI): 496.0342 [M + H]$^+$; Calcd for $C_{21}H_{13}N_3O_4SF_3Cl$: 496.0340.

6-Chloro-3-nitro-2-(phenylsulfonylmethyl)-8-(3-trifluoromethylphenyl)imidazo[1,2-*a*]pyridine (20): Compound **20** was obtained after purification by chromatography (eluent: dichloromethane/cyclohexane/diethyl ether 5.5/4/0.5) and recrystallization from acetonitrile as a yellow solid in 59% yield (0.27 g). mp 182 °C; ^{1}H NMR (400 MHz, [D$_6$]DMSO) δ: 5.28 (s, 2H), 7.32–7.39 (m, 1H), 7.56–7.70 (m, 3H), 7.74–7.86 (m, 3H), 7.93–7.96 (m, ^{1}H), 8.20–8.27 (m, 2H), 9.41 (s, 1H); ^{13}C NMR (100 MHz, [D$_6$]DMSO) δ: 55.7 (CH_2), 124.0 (q, J = 272.4 Hz, CF_3), 124.4 (C), 125.4 (CH), 125.9 (q, J = 3.9 Hz, 2CH), 128.2 (2CH), 128.5 (C), 129.2 (2CH), 129.3 (CH), 129.4 (q, J = 32 Hz, C), 131.0 (CH), 131.1 (C), 133.6 (CH), 133.9 (C), 134.1 (CH), 138.7 (C), 139.4 (C), 141.0 (C); MS ESI$^+$ (m/z): 495.82/497.89 [M +H]$^+$; HRMS (+ESI): 496.0340 [M + H]$^+$; Calcd for $C_{21}H_{13}N_3O_4SF_3Cl$: 496.0340.

6-Chloro-3-nitro-2-(phenylsulfonylmethyl)-8-(2-trifluoromethylphenyl)imidazo[1,2-*a*]pyridine (21): Compound **21** was obtained after purification by chromatography (eluent: dichloromethane/cyclohexane/diethyl ether 5/4.5/0.5) and recrystallization from propan-2-ol as a yellow solid in 41% yield (0.19 g). mp 189 °C; ^{1}H NMR (300 MHz, [D$_6$]DMSO) δ: 5.21 (s, 2H), 7.37–7.39 (m, 1H), 7.51–7.55 (m, 2H), 7.65–7.67 (m, 2H), 7.70–7.79 (m, 3H), 7.88–7.89 (m, 1H), 7.92 (s, 1H), 9.44 (s, 1H); ^{13}C NMR (75 MHz, [D$_6$] DMSO) δ: 55.6 (CH_2), 123.4 (C), 123.7 (q, J = 274.3 Hz, CF_3), 125.8 (CH), 126.2 (q, J = 4.9 Hz, CH), 127.6 (q, J = 29.8 Hz, C), 128.3 (2CH), 128.8 (C), 129.0 (2CH), 129.6 (CH), 131.1 (C), 131.7 (d, J = 2.1 Hz, C), 131.9 (d, J = 1.3 Hz, CH), 132.1 (CH), 132.6 (CH), 134.0 (CH), 138.5 (C), 139.5 (C), 141.8 (C); MS ESI$^+$ (m/z): 495.78/497.89 [M+H]$^+$; HRMS (+ESI): 496.0341 [M + H]$^+$; Calcd for $C_{21}H_{13}N_3O_4SF_3Cl$: 496.0340.

6-Chloro-3-nitro-2-(phenylsulfonylmethyl)-8-(pyridin-3-yl) imidazo[1,2-*a*]pyridine (22): Compound **22** was obtained after purification by chromatography (eluent: dichloromethane/ethyl acetate 9/1) and recrystallization from acetonitrile as a yellow solid in 53% yield (0.21 g). mp 215 °C; ^{1}H NMR (400 MHz, [D$_6$]DMSO) δ: 5.30 (s, 2H), 7.44–7.50 (m, 1H), 7.59–7.65 (m, 2H), 7.77–7.83 (m, 3H), 7.99–8.02 (m, 1H), 8.25 (s, 1H), 8.66 (d, J = 4.5 Hz, 1H), 8.92 (s, 1H), 9.40 (s, 1H); ^{13}C NMR (100 MHz, [D$_6$]DMSO) δ: 55.6 (CH_2), 123.2 (CH), 124.4 (C), 125.4 (CH), 127.2 (C), 128.3 (2CH), 128.9 (C), 129.3 (2CH), 130.6 (CH), 131.1 (C), 134.2 (CH), 136.8 (CH), 138.6 (C), 139.4 (C), 141.0 (C), 149.6 (CH), 150.1 (CH); MS ESI$^+$ (m/z): 428.95/430.89 [M+H]$^+$; HRMS (+ESI): 429.0418 [M + H]$^+$; Calcd for $C_{19}H_{13}N_4O_4SCl$: 429.0419.

6-Chloro-3-nitro-2-(phenylsulfonylmethyl)-8-(pyridin-4-yl) imidazo[1,2-*a*]pyridine (23): Compound **23** was obtained after purification by chromatography (eluent: dichloromethane/ethyl acetate 9/1) and recrystallization from acetonitrile as a yellow solid in 51% yield (0.20 g). mp 230 °C; ^{1}H NMR (400 MHz, $CDCl_3$) δ: 5.18 (s, 2H), 7.52–7.58 (m,

2H), 7.67–7.74 (m, 3H), 7.82–7.89 (m, 3H), 8.73 (d, J = 5.5 Hz, 2H), 9.54 (s, 1H); ^{13}C NMR (100 MHz, $CDCl_3$) δ: 56.6 (CH_2), 123.6 (2CH), 125.7 (C), 126.0 (CH), 128.7 (2CH), 128.8 (C), 129.4 (2CH), 130.8 (CH), 131.3 (C), 134.3 (CH), 139.4 (C), 139.8 (C), 140.8 (C), 141.2 (C), 150.3 (2CH); MS ESI$^+$ (m/z): 428.93/430.97 $[M+H]^+$; HRMS (+ESI): 429.0417 $[M + H]^+$; Calcd for $C_{19}H_{13}N_4O_4SCl$: 429.0419.

6-Chloro-3-nitro-2-(phenylsulfonylmethyl)-8-(thiophen-2-yl)imidazo[1,2-*a*]pyridine (24): Compound **24** was obtained after purification by chromatography (eluent: dichloromethane/cyclohexane/diethyl ether 5.5/4/0.5) as a yellow solid in 60% yield (0.24 g). mp 255 °C; ^{1}H NMR (300 MHz, $[D_6]$DMSO) δ: 5.33 (s, 2H), 7.21 (s, 1H), 7.61–7.99 (m, 7H), 8.30 (s, 1H), 9.26 (s, 1H); ^{13}C NMR (75 MHz, $[D_6]$DMSO) δ: 55.7 (CH_2), 123.8 (CH), 123.9 (C), 124.4 (C), 126.9 (CH), 127.8 (CH), 128.2 (2CH), 129.4 (2CH), 129.7 (CH), 130.6 (CH), 131.6 (C), 133.8 (C), 134.2 (CH), 138.8 (C), 138.9 (C), 141.1 (C); MS ESI$^+$ (m/z): 433.81/435.84 $[M+H]^+$; HRMS (+ESI): 434.0050 $[M + H]^+$; Calcd for $C_{18}H_{12}ClN_3O_4S_2$: 434.0031.

6-Chloro-8-(furan-2-yl)-3-nitro-2-(phenylsulfonylmethyl)imidazo[1,2-*a*]pyridine (25): Compound **25** was obtained after purification by chromatography (eluent: dichloromethane/cyclohexane/diethyl ether 4/5.5/0.5) and recrystallization from acetonitrile as a yellow solid in 53% yield (0.21 g). mp 236 °C; ^{1}H NMR (400 MHz, $[D_6]$DMSO) δ: 5.34 (s, 2H), 6.70 (q, J = 1.8 Hz, 1H), 7.10 (d, J = 3.1 Hz, 1H), 7.57–7.62 (m, 2H), 7.75 (tt, J = 1.2 Hz and 7.5 Hz, 1H), 7.81–7.84 (m, 2H), 7.97 (dd, J = 0.6 Hz and 1.7 Hz, 1H), 8.02 (d, J = 1.9 Hz, 1H), 9.23 (d, J = 1.9 Hz, 1H); ^{13}C NMR (100 MHz, $[D_6]$ DMSO) δ: 55.6 (CH_2), 112.7 (CH), 114.9 (CH), 119.6 (C), 123.7 (CH), 124.2 (C), 124.3 (CH), 128.2 (2CH), 129.2 (2CH), 131.2 (C), 134.1 (CH), 138.3 (C), 138.8 (C), 139.0 (C), 145.5 (C), 145.6 (CH); MS ESI$^+$ (m/z): 417.01/418.25 $[M+H]^+$; HRMS (+ESI): 418.0254 $[M + H]^+$; Calcd for $C_{18}H_{12}N_3O_5SCl$: 418.0259.

3.1.2 Biology—Antileishmanial activity assay on *L. infantum* axenic amastigotes

[32]: *L. infantum* promastigotes in logarithmic phase were centrifuged at 900 G for 10 min. The supernatant was removed carefully and replaced by the same volume of RPMI 1640 complete medium at pH 5.4 and incubated for 24 h at 24 °C. The acidified promastigotes were incubated for 24 h at 37 °C in a ventilated flask. Promastigotes were then transformed into amastigotes. The effects of the tested compounds on the growth of *L. infantum* axenic amastigotes were assessed as follows. *L. infantum* amastigotes were incubated at a density of 2.106 parasites/mL in sterile 96-well plates with various concentrations of compounds dissolved in DMSO (final concentration less than 0.5% v/v), in duplicate. Appropriate controls (DMSO, amphotericin B, miltefosine and pentamidine) were added to each set of experiments. After a 48 h incubation period at 37 °C, each plate-well was microscope-examined for detecting any precipitate formation. To estimate the luciferase activity of axenic amastigotes, 80 µL of each well were transferred to white 96-well plates, Steady Glow® reagent (Promega) was added according to manufacturer's instructions, and plates were incubated for 2 min. The luminescence was measured in Microbeta Luminescence Counter (PerkinElmer). Inhibitory concentration 50% (IC_{50}) was defined as the concentration of drug required to inhibit by 50% the metabolic activity of *L. infantum* amastigotes compared to control. IC_{50} values were calculated by non-linear regression

analysis processed on dose-response curves, using TableCurve 2D V5 software. IC_{50} values represent the mean.

Antileishmanial activity assay on *L. donovani* promastigotes: The effects of the tested compounds on the growth of *L. donovani* promastigotes (MHOM/IN/00/DEVI strain) were assessed by MTT assay [33]. Briefly, promastigotes in log-phase in Schneider's medium supplemented with 20% fœtal calf serum (FCS), 2 mM L-glutamine and antibiotics (100 U/mL penicillin and 100 μg mL^{-1} streptomycin), were incubated at an average density of 10^6 parasites/mL in sterile 96-well plates with various concentrations of compounds dissolved in DMSO (final concentration less than 0.5% v/v), in duplicate. Appropriate controls treated by DMSO, miltefosine or amphotericin B (reference drugs purchased from Sigma Aldrich) were added to each set of experiments. After a 72 h incubation period at 27 °C, parasite metabolic activity was determined. Each plate-well was then microscope-examined for detecting possible precipitate formation. 10 μL of MTT (3-(4,5-dimethylthiazol-2-yl)-2,5-diphenyltetrazolium bromide) solution (10 mg/mL in PBS) were added to each well followed by incubation for another 4 h. The enzyme reaction was then stopped by addition of 100 μL of 50% isopropanol–10% sodium dodecyl sulfate. The plates were shaken vigorously (300 rpm) for 10 min. The absorbance was finally measured at 570 nm in a BIO-TEK ELx808 Absorbance Microplate Reader. Inhibitory concentration 50% (IC_{50}) was defined as the concentration of drug required to inhibit by 50% the metabolic activity of *L. donovani* and promastigotes compared to the control. IC_{50} were calculated by nonlinear regression analysis processed on dose–response curves, using TableCurve 2D V5.0 software. IC_{50} values represent the mean value calculated from three independent experiments.

Antileishmanial activity assay on *L. donovani* intramacrophage amastigotes: The effects of the tested compounds on the growth of *Leishmania donovani* amastigotes were assessed according to the method of da Luz et al. [34]. 400 μL of THP-1 cells with Phorbol 12-Myristate 13-Acetate (final concentration: 50 ng/mL) were seeded in sterile chamber-slides at an average density of 10^5 cells/mL and incubated for 48 h at 37 °C and 6% CO_2. *L. donovani* promastigotes were centrifuged at 900 G for 10 min and the supernatant was replaced by the same volume of Schneider 20% FCS pH 5.4 and incubated for 24 h at 27 °C. THP-1 cells were then infected by acidified promastigotes at an average density of 10^6 cells/mL (10:1 ratio) and chamber-slides were incubated for 24 h at 37 °C. Then, in duplicate, the medium containing various concentrations of tested compounds was added (final DMSO concentration below 0.5% v/v). Appropriate controls treated with or without solvent (DMSO), and various concentrations of miltefosine and amphotericin B were added to each set of experiments. After a 120 h incubation at 37 °C and 6% CO_2, the well supernatant was removed. Cells were fixed with analytical grade methanol and stained with 10% Giemsa. The percentage of infected macrophages in each assay was determined microscopically by counting at least 200 cells in each sample. IC_{50} was defined as the concentration of drug necessary to produce a 50% decrease in infected macrophages compared to the control. IC_{50} were calculated by non-linear regression analysis processed on dose–response curves, using TableCurve 2D V5.0 software. IC_{50} values represent the mean value calculated from three independent experiments.

Antitrypanosomal activity assay on trypomastigotes: The effects of the tested compounds on the growth of *T. brucei brucei* were assessed by Alamar Blue® assay described by Räz et al. [35] *Trypanosoma brucei brucei* AnTat 1.9 (IMTA, Antwerpen, Belgium) was cultured in MEM with Earle's salts, supplemented according to the protocol of Baltz et al. [36] with the following modifications: 0.5 mM Mercaptoethanol (Sigma Aldrich®, France), 1.5 mM L-cysteine (Sigma Aldrich®), 0.05 mM Bathocuproïne sulfate (Sigma Aldrich®) and 20% heat-inactivated horse serum (Gibco®, France), at 37 °C and 5% CO_2. They were incubated at an average density of 2000 parasites/100 μL in sterile 96-well plates (Fisher®, France) with various concentrations of compounds dissolved in DMSO, in duplicate. Appropriate controls treated by DMSO on sterile water, suramin, eflornithine and fexinidazole (reference drugs purchased from Sigma Aldrich, France and Fluorochem, UK) were added to each set of experiments. After a 69 h incubation period at 37 °C, 10 μL of the viability marker Alamar Blue® (Fisher, France) was then added to each well, and the plates were incubated for 5 h. The plates were read in a PerkinElmer ENSPIRE (Germany) microplate reader using an excitation wavelength of 530 nm and an emission wavelength of 590 nm. IC_{50} was defined as the concentration of drug necessary to inhibit by 50% the activity of *T. brucei brucei* compared to the control. IC_{50} were calculated by nonlinear regression analysis processed on dose-response curves, using GraphPad Prism software (USA). IC_{50} values were calculated from three independent experiments.

Cytotoxicity assay on HepG2 cell line: The evaluation of the tested molecules cytotoxicity on the HepG2 cell line (hepatocarcinoma cell line purchased from ATCC, ref H-8065) was performed according to the method of Mosman [33] with slight modifications. Briefly, cells in 100 μL of complete RPMI medium, [RPMI supplemented with 10% FCS, 1% L-glutamine (200 mM) and penicillin (100 U/mL)/streptomycin (100 μg mL^{-1})] were inoculated into each well of 96-well plates and incubated at 37 °C in a humidified 6% CO_2. After a 24 h incubation, 100 μL of medium with various product concentrations dissolved in DMSO (final concentration less than 0.5% v/v) were added and the plates were incubated for 72 h at 37 °C. Duplicate assays were performed for each sample. Each plate-well was then microscope-examined for detecting possible precipitate formation before the medium was aspirated from the wells. 100 μL of MTT solution (0.5 mg/mL in medium without FCS) were then added to each well. Cells were incubated for 2 h at 37 °C. After this time, the MTT solution was removed and DMSO (100 μL) was added to dissolve the resulting blue formazan crystals. Plates were shaken vigorously (300 rpm) for 5 min. The absorbance was measured at 570 nm with 630 nm as reference wavelength spectrophotometer using a BIO-TEK ELx808 Absorbance Microplate Reader. DMSO was used as blank and doxorubicin (purchased from Sigma Aldrich) as positive control. Cell viability was calculated as percentage of control (cells incubated without compound). The 50% cytotoxic concentration was determined from the dose–response curve by using the TableCurve 2D V5.0 software.

Cytotoxicity assay on THP1 cell line: The evaluation of the tested molecules cytotoxicity on the differentiated THP1 cell line (acute monocyte leukemia cell line purchased from ATCC, ref TIB-202) was performed according to the method of Mosman [33] with slight modifications. Briefly, cells in 100 μL of complete RPMI medium with Phorbol 12-myristate 13-acetate (final concentration: 50 ng/mL) were incubated at an average density of 10^6

cells/mL and in sterile 96-well plates. After a 48 h incubation, 100 μL of medium with various product concentrations dissolved in DMSO (final concentration less than 0.5% v/v) were added and the plates were incubated for 72 h at 37 °C. Each plate-well was then microscope-examined for detecting possible precipitate formation before the medium was aspirated from the wells. 100 μL of MTT solution (0.5 mg/mL in medium without FCS) were then added to each well. Cells were incubated for 2 h at 37 °C. After this time, the MTT solution was removed and DMSO (100 μL) was added to dissolve the resulting blue formazan crystals. Plates were shaken vigorously (300 rpm) for 10 min. The absorbance was measured at 570 nm with 630 nm as reference wavelength spectrophotometer using a BIO-TEK ELx808 Absorbance Microplate Reader. DMSO was used as blank and doxorubicin (purchased from Sigma Aldrich) as positive control. Cell viability was calculated as percentage of control (cells incubated without compound). The 50% cytotoxic concentration was determined from the dose–response curve by using the TableCurve 2D V5.0 software.

Metabolism of 13 and 23 in *L. donovani* promastigotes: The clonal *Leishmania donovani* cell line LdBOB (derived from MHOM/SD/62/1S-CL2D) was grown as promastigotes at 26 °C in modified M199 media, as previously described [37]. LdBOB promastigotes overexpressing NTR1 (LinJ.05.0660) [19] and NTR2 (LinJ.12.0730) [20] were grown in the presence of nourseothricin (100 μg mL^{-1}). Then to examine the effects of test compounds on growth, triplicate promastigote cultures were seeded with 5×10^4 parasites.mL^{-1}. Parasites were grown in 10 mL cultures in the presence of drug for 72 h, after which 200 μL aliquots of each culture were added to 96-well plates, 50 μM resazurin was added to each well and fluorescence (excitation of 528 nm and emission of 590 nm) measured after a further 4 h incubation [14]. Data were processed using GRAFIT (version 5.0.4; Erithacus software) and fitted to a 2-parameter equation, where the data are corrected for background fluorescence, to obtain the effective concentration inhibiting growth by 50% (EC_{50}):

$$y = \frac{100}{1 + \left(\frac{[I]}{EC_{50}}\right)^m}$$

In this equation [I] represents inhibitor concentration and m is the slope factor. Experiments were repeated at least two times and the data is presented as the mean plus standard deviation.

Metabolism of 14 and 20 in *T. brucei*: *Trypanosoma brucei* bloodstream-form 'single marker' S427 (T7RPOL TETR NEO) and drug-resistant cell lines were cultured at 37 °C in HMI9-T medium [38] supplemented with 2.5 μg mL^{-1} G418 to maintain expression of T7 RNA polymerase and the tetracycline repressor protein. Bloodstream trypanosomes overexpressing the *T. brucei* nitroreductase (NTR1) [21] were grown in medium supplemented with 2.5 μg mL^{-1} phleomycin and expression of NTR was induced by the addition of 1 μg mL^{-1} tetracycline. Cultures were initiated with 1×10^5 cells.mL^{-1} and sub-cultured when cell densities approached 1–2 ($\times 10^6$).mL^{-1}.

In order to examine the effects of inhibitors on the growth of these parasites, triplicate cultures containing the inhibitor were seeded at 1×10^5 trypanosomes.mL^{-1}. Cells

overexpressing NTR were induced with tetracycline 48 h prior to EC_{50} analysis. Cell densities were determined after culture for 72 h, as previously described [39]. EC_{50} values were determined using the following two-parameter equation by non-linear regression using GraFit:

where the experimental data were corrected for background cell density and expressed as a percentage of the uninhibited control cell density.

$$y = \frac{100}{1 + \left(\frac{[I]}{EC_{50}}\right)^{m}}$$

In this equation [I] represents inhibitor concentration and m is the slope factor.

Supplementary Material

Refer to Web version on PubMed Central for supplementary material.

Acknowledgements

This work is supported by Aix-Marseille Université, the Université de Toulouse and the CNRS. A. Fairlamb and S. Wyllie are supported by funding from the Wellcome Trust (WT105021). C. Fersing thanks the Assistance Publique - Hôpitaux de Marseille (AP-HM) for hospital appointment. The authors thank Dr Vincent Remusat for the NMR spectra recording, Christophe Chendo and Valérie Monnier for the HRMS analyses and Dr Michel Giorgi for the X-ray structure determinations.

References

[1]. World Health Organization (WHO). www.who.int/neglected_diseases/diseases/en

[2]. Molyneux DH, Savioli L, Engels D. Lancet. 2017; 389:312–325. [PubMed: 27639954]

[3]. World Health organization (WHO). www.who.int/leishmaniasis/en/

[4]. Pace D. J Infect. 2014; 69:s10–s18. [PubMed: 25238669]

[5]. World Health organization (WHO). www.who.int/trypanosomiasis_african/en/

[6]. Büscher P, Cecchi G, Jamonneau V, Priotto G. Lancet. 2017; 390:2397–2409. [PubMed: 28673422]

[7]. Sundar S, Singh A. Parasitology. 2017; doi: 10.1017/S0031182017002116

[8]. Kennedy PGE. Lancet Neurol. 2013; 12:186–194. [PubMed: 23260189]

[9]. Field MC, Horn D, Fairlamb AH, Ferguson MA, Gray DW, Read KD, de Rycker M, Torrie LS, Wyatt PG, Wyllie S, Gilbert IH. Nat Rev Microbiol. 2017; 15:217–231. [PubMed: 28239154]

[10]. Nagle AS, Khare S, Kumar AB, Supek F, Buchynskyy A, Mathison CJ, Chennamaneni NK, Pendem N, Buckner FS, Gelb MH, Molteni V. Chem Rev. 2014; 114:11305–11347. [PubMed: 25365529]

[11]. Drugs for neglected diseases initiative (DNDi). www.dndi.org/diseases-projects/portfolio/

[12]. Mesu VKBK, Kalonji WM, Bardonneau C, Mordt OV, Blesson S, Simon F, Mbembo HM, Ilunga M, Bonama AK, Heradi JA, Solomo JLL, et al. Lancet. 2018; 391:144–154. [PubMed: 29113731]

[13]. Patterson S, Wyllie S, Norval S, Stojanovski L, Simeons FRC, Auer JL, Osuna-Cabello M, Read KD, Fairlamb AH. eLife. 2016; 5:e09744. [PubMed: 27215734]

[14]. Wyllie S, Patterson S, Stojanovski L, Simeons FRC, Norval S, Kime R, Read KD, Fairlamb AH. Sci Transl Med. 2012; 4

[15]. Torreele E, Bourdin Trunz B, Tweats D, Kaiser M, Brun R, Mazué G, Bray MA, Pécoul B. PLoS Neglected Trop Dis. 2010; 4:e923.

[16]. Kaiser M, Bray MA, Cal M, Bourdin Trunz B, Torreele E, Brun R. Antimicrob Agents Chemother. 2011; 55:2602–5608.

[17]. Patterson S, Wyllie S. Trends Parasitol. 2014; 30:289–298. [PubMed: 24776300]

[18]. Voak AA, Gobalakrishnapillai V, Seifert K, Balczo E, Hu L, Hall BS, Wilkinson SR. J Biol Chem. 2013; 288:28466–28476. [PubMed: 23946481]

[19]. Wyllie S, Patterson S, Fairlamb A. Antimicrob Agents Chemother. 2013; 57:901–906. [PubMed: 23208716]

[20]. Wyllie S, Roberts AJ, Norval S, Patterson S, Foth B, Berriman M, Read K, Fairlamb AH. PLoS Pathog. 2016; 12

[21]. Wyllie S, Foth BJ, Kelner A, Sokolova AY, Berriman M, Fairlamb AH. J Antimicrob Chemother. 2016; 71:625–634. [PubMed: 26581221]

[22]. Marhadour S, Marchand P, Pagniez F, Bazin M-A, Picota C, Lozach O, Ruchaud S, Antoine M, Meijer L, Rachidi N, Le Pape P. Eur J Med Chem. 2012; 58:543–556. [PubMed: 23164660]

[23]. Castera-Ducros C, Paloque L, Verhaeghe P, Casanova M, Cantelli C, Hutter S, Tanguy F, Laget M, Remusat V, Cohen A, Crozet MD, et al. Bioorg Med Chem. 2013; 21:7155–7164. [PubMed: 24080103]

[24]. Kieffer C, Cohen A, Verhaeghe P, Paloque L, Hutter S, Castera-Ducros C, Laget M, Rault S, Valentin A, Rathelot P, Azas N, et al. Bioorg Med Chem. 2015; 23:2377–2386. [PubMed: 25846065]

[25]. Marie E, Bouclé S, Enguehard-Gueiffier C, Gueiffier A. Molecules. 2012; 17:10683–10707. [PubMed: 22955457]

[26]. Szabo R, Crozet MD, Vanelle P. Synthesis. 2008:127–135.

[27]. Castera C, Crozet MD, Vanelle P. Heterocycles. 2005; 65:2979–2989.

[28]. Crozet MD, Castera-Ducros C, Vanelle P. Tetrahedron Lett. 2006; 47:7061–7065.

[29]. Kabri Y, Verhaeghe P, Gellis A, Vanelle P. Molecules. 2010; 15:2949. [PubMed: 20657457]

[30]. Katsuno K, Burrows JN, Duncan K, van Huijsduijnen RH, Kaneko T, Kita K, Mowbray CE, Schmatz D, Warner P, Slingsby BT. Nat Rev Drug Discov. 2015; 14:751–758. [PubMed: 26435527]

[31]. Mattern G. Helv Chim Acta. 1977; 60:2062–2070.

[32]. Zhang C, Bourgeade-Delmas S, Alvarez AF, Valentin A, Hemmert C, Gornitzka H. Eur J Med Chem. 2018; 143:1635–1643. [PubMed: 29133045]

[33]. Mossmann TJ. J Immunol Meth. 1983; 65:55–63.

[34]. da Luz RI, Vermeersch M, Dujardin J-C, Cos P, Maes L. Antimicrob Agents Chemother. 2009; 53:5197–5203. [PubMed: 19752271]

[35]. Räz B, Iten M, Grether-Bühler Y, Kaminsky R, Brun R. Acta Trop. 1997; 68:139–147. [PubMed: 9386789]

[36]. Baltz T, Baltz D, Giroud C, Crockett J. EMBO J. 1985; 4:1273–1277. [PubMed: 4006919]

[37]. Goyard S, Segawa H, Gordon J, Showalter M, Duncan R, Turco SJ, Beverley SM. Mol Biochem Parasitol. 2003; 130:31–42. [PubMed: 14550894]

[38]. Greig N, Wyllie S, Patterson S, Fairlamb AH. FEBS J. 2009; 276:376–386. [PubMed: 19076214]

[39]. Jones DC, Hallyburton I, Stojanovski L, Read KD, Frearson JA, Fairlamb AH. Biochem Pharmacol. 2010; 80:1478–1486. [PubMed: 20696141]

Europe PMC Funders Author Manuscripts

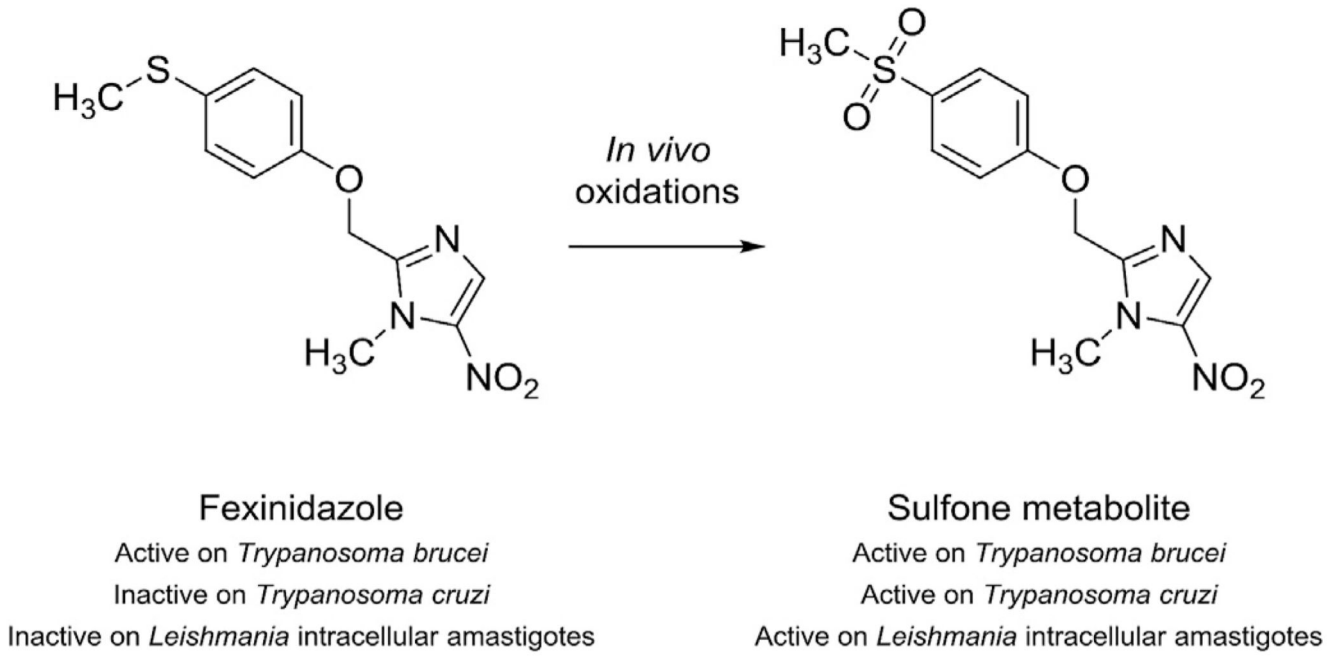

Fig. 1.
Structure of drug candidate fexinidazole and its active sulfone metabolite.

Europe PMC Funders Author Manuscripts

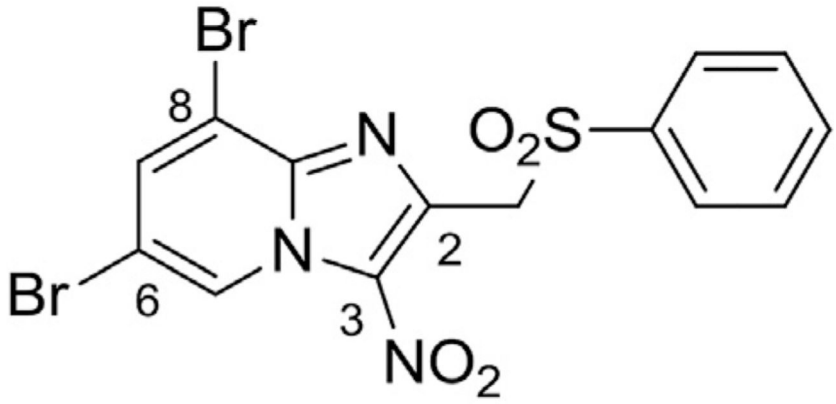

Initial antileishmanial hit molecule

IC_{50} *L. donovani* promastigotes = 1.8 μM

IC_{50} *L. donovani* intramacrophage amastigotes = 5.5 μM

CC_{50} HepG2 > 31 μM / CC_{50} THP1 > 25 μM

Fig. 2.

Structure, *in vitro* antileishmanial activity and cytotoxicity of the previously identified hit molecule 6,8-dibromo-3-nitro-2-(phenylsulfonylmethyl)imidazo[1,2-*a*]pyridine.

Europe PMC Funders Author Manuscripts

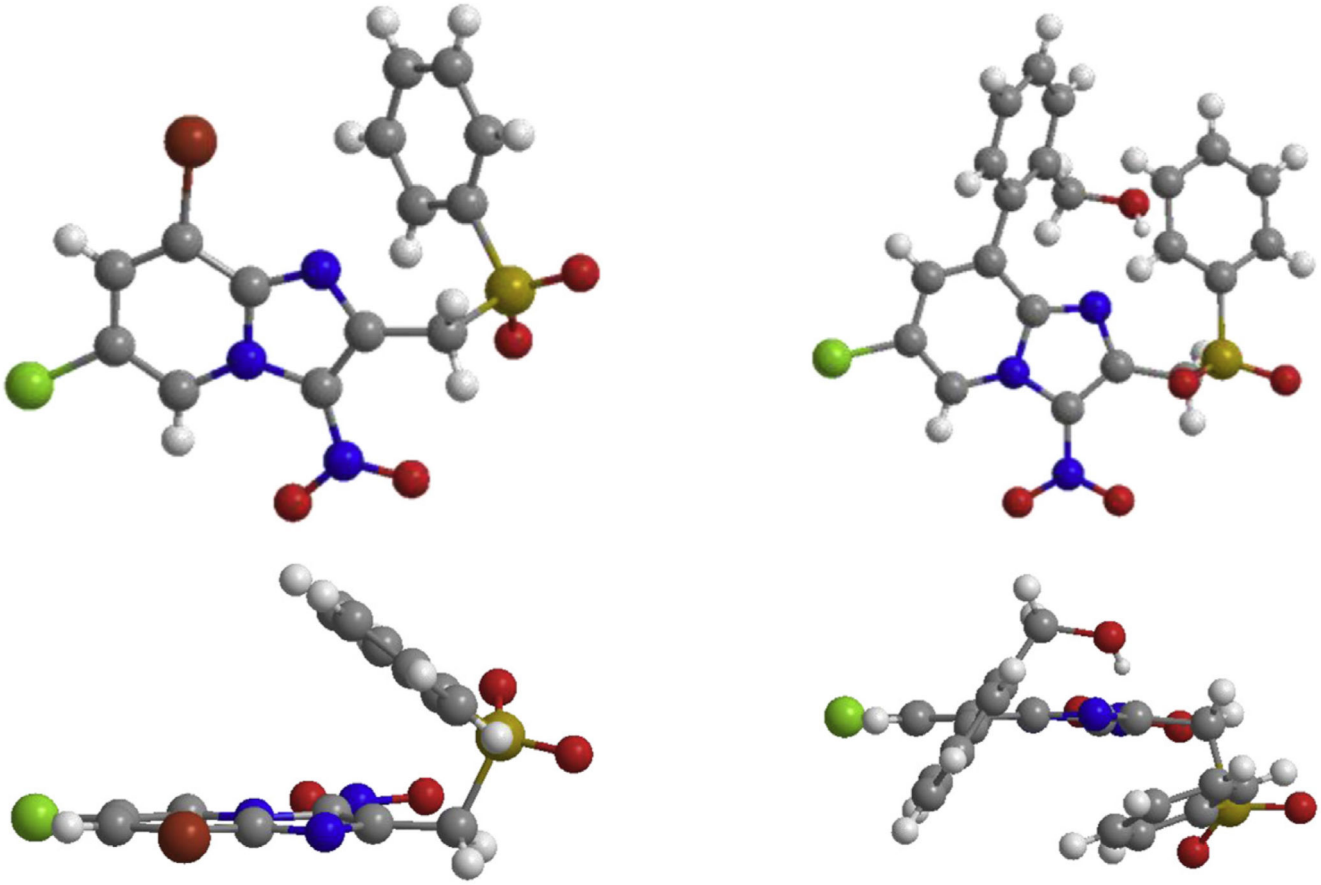

Fig. 3.
X-ray structures of compounds **4** (left) and **14** (right).

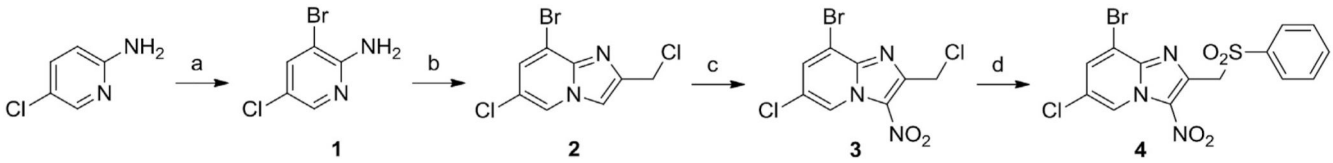

Scheme 1.

Synthesis of substrate **4**: a) NBS, acetonitrile, 80 °C, 1 h, 71%; b) 1,3-dichloroacetone, EtOH, 80 °C, 96 h, 60%; c) HNO_3, H_2SO_4, 0 °C→RT, 1 h, 60%; d) Sodium benzenesulfinate, DMSO, RT, 3 h, 80%.

Europe PMC Funders Author Manuscripts

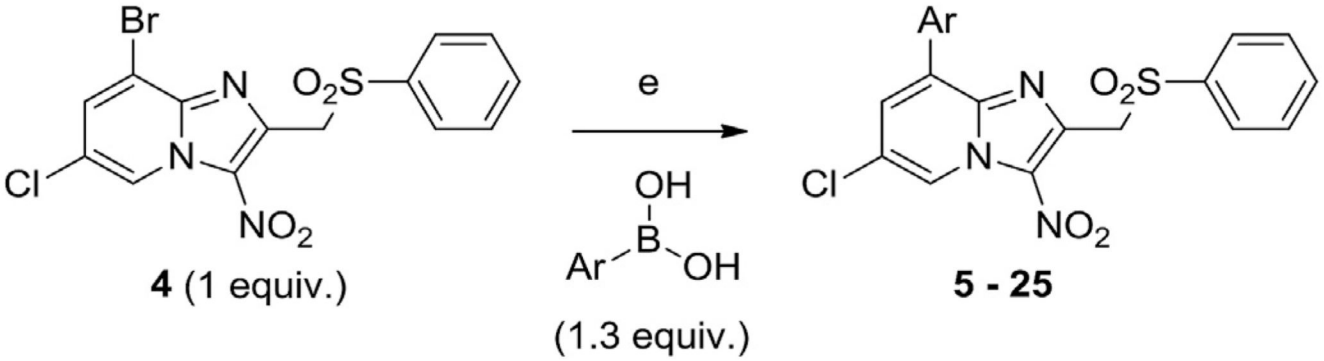

Scheme 2.

General procedure for the Suzuki-Miyaura cross-coupling reaction between imidazo[1,2-*a*]pyridine derivative **4** and various aryl- or heteroarylboronic acids using the optimized protocol: e) 0.1 equiv. of $Pd(PPh_3)_4$, 5 equiv. of K_2CO_3, THF in sealed tube, 120 °C, MW, 30 min to 2 h, 41%–90% yield.

Table 1

Optimization of the Suzuki-Miyaura cross-coupling reaction between substrate 4 and phenylboronic acid.

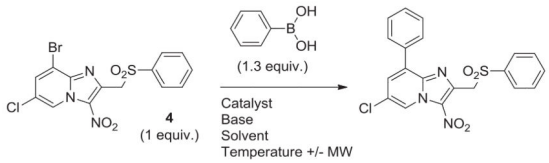

Entry	Reactant (1.3 equiv.)	Solvent	Base	Catalyst	Temp (°C)	Time (h)	Yield[a] (%)
1	Ph-B(OH)$_2$	Dioxane	Na_2CO_3, 3 equiv.	Pd(PPh$_3$)$_4$; 0.1 equiv.	110	24	*b*
2	Ph-B(OH)$_2$	DME	Na_2CO_3, 3 equiv.	Pd(PPh$_3$)$_4$; 0.1 equiv.	85, MW	2	*b*
3	Ph-B(OH)$_2$	Dioxane	Na_2CO_3, 5 equiv.	Pd(PPh$_3$)$_4$; 0.1 equiv.	110	24	47
4	Ph-B(OH)$_2$	DME	Na_2CO_3, 5 equiv.	Pd(PPh$_3$)$_4$; 0.1 equiv.	85, MW	2	49
5	Ph-B(OH)$_2$	THF	Na_2CO_3, 5 equiv.	Pd(PPh$_3$)$_4$; 0.1 equiv.	70, MW	3	*b*
6	Ph-B(OH)$_2$	Water	Na_2CO_3, 5 equiv.	Pd(PPh$_3$)$_4$; 0.1 equiv.	100	24	*b*
7	Ph-B(OH)$_2$	Water + TBAB	Na_2CO_3, 5 equiv.	Pd(PPh$_3$)$_4$; 0.1 equiv.	100, MW	3	*b*
8	Ph-B(OH)$_2$	Water/EtOH (8:2)	Na_2CO_3, 5 equiv.	Pd(PPh$_3$)$_4$; 0.1 equiv.	90, MW	3	*b*
9	Ph-B(OH)$_2$	Water/EtOH (5:5)	Na_2CO_3, 5 equiv.	Pd(PPh$_3$)$_4$; 0.1 equiv.	90, MW	3	40
10	Ph-B(OH)$_2$	DME/Water (9:1)	Na_2CO_3, 5 equiv.	Pd(PPh$_3$)$_4$; 0.1 equiv.	85, MW	3	*b*
11	Ph-B(OH)$_2$	DME	Cs_2CO_3, 3 equiv.	Pd(PPh$_3$)$_4$; 0.1 equiv.	85, MW	1.5	25
12	Ph-B(OH)$_2$	DME	K_3PO_4, 5 equiv.	Pd(PPh$_3$)$_4$; 0.1 equiv.	85, MW	3	20
13	Ph-B(OH)$_2$	DME	CsF, 5 equiv.	Pd(PPh$_3$)$_4$; 0.1 equiv.	85, MW	3	*b*
14	Ph-B(OH)$_2$	DME	K_2CO_3, 3 equiv.	Pd(PPh$_3$)$_4$; 0.1 equiv.	85, MW	3	*b*
15	Ph-B(OH)$_2$	DME	K_2CO_3, 4 equiv.	Pd(PPh$_3$)$_4$; 0.1 equiv.	85, MW	3	*b*
16	Ph-B(OH)$_2$	DME	K_2CO_3, 5 equiv.	Pd(PPh$_3$)$_4$; 0.1 equiv.	85, MW	3	64
17	Ph-B(OH)$_2$	DME	K_2CO_3, 5 equiv.	Pd(dppf)Cl$_2$; 0.1 equiv.	85, MW	3	53
18	Ph-B(OH)$_2$	DME	K_2CO_3, 5 equiv.	PdCl$_2$(PPh$_3$)$_2$; 0.1 equiv.	85, MW	3	51
19	Ph-B(OH)$_2$	DME	K_2CO_3, 5 equiv.	Pd(OAc)$_2$; 0.1 equiv.	85, MW	3	58
20	Ph-B(OH)$_2$	DME	K_2CO_3, 5 equiv.	Pd(PPh$_3$)$_4$; 0.1 equiv.	85	6	49
21	Ph-B(OH)$_2$	DME	K_2CO_3, 5 equiv.	Pd(PPh$_3$)$_4$; 0.1 equiv.	95, MW	2	58
22	Ph-B(OH)$_2$	THF	K_2CO_3, 5 equiv.	Pd(PPh$_3$)$_4$; 0.1 equiv.	70	36	73
23	Ph-B(OH)$_2$	THF	K_2CO_3, 5 equiv.	Pd(PPh$_3$)$_4$; 0.1 equiv.	70, MW	3	*b*
24	Ph-B(OH)$_2$	THF	K_2CO_3, 5 equiv.	Pd(PPh$_3$)$_4$; 0.1 equiv.	90, MW	5	90
25	**Ph-B(OH)$_2$**	**THF**	**K_2CO_3, 5 equiv.**	**Pd(PPh$_3$)$_4$; 0.1 equiv.**	**120, MW**	**1**	**90**
26	Ph-B(OH)$_2$	THF	K_2CO_3, 5 equiv.	Pd(PPh$_3$)$_4$; 0.05 equiv.	120, MW	1	36
27	*4-CH$_3$O-Ph-B(OH)$_2$*	*THF*	*K_2CO_3, 5 equiv.*	*Pd(PPh$_3$)$_4$; 0.1 equiv.*	*120, MW*	*2*	***84***
28	*4-CF$_3$-Ph-B(OH)$_2$*	*THF*	*K_2CO_3, 5 equiv.*	*Pd(PPh$_3$)$_4$; 0.1 equiv.*	*120, MW*	*1*	***87***

In bold: Best reaction conditions.

[a]The reaction yield was calculated form the product isolated after purification by chromatography column.

[b]Only partial conversion of starting material was observed on TLC.

Table 2

In vitro **antileishmanial (*L. infantum*) and antitrypanosomal screening and cytotoxicity of synthesized imidazo[1,2-*a*]pyridine derivatives (5-25).**

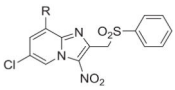

Compd	R-	CC_{50} HepG2 (μM)	IC_{50} *L. infantum* axenic amastigotes (μM)	*Selectivity Index (SI) Leishmania*[f]	IC_{50} *T. brucei brucei* trypomastigotes (μM)	*Selectivity Index (SI) Trypanosoma*[g]	cLogP[h]
5	**Ph-**	**>15.6**[d]	**1.6 ± 0.6**	**>10**	0.61 ± 0.2	>25.6	4.1
6	4-Cl-Ph-	>3.9[d]	–	–	–	–	4.8
7	4-CH_3O-Ph-	>3.9[d]	–	–	–	–	4.0
8	4-$((C_2H_5)_2N)$-Ph-	>15.6[d]	2.5 ± 0.5	>6.2	0.43 ± 0.06	>36.3	5.0
9	4-CN-Ph-	>3.9[d]	–	–	–	–	4.0
10	**4-CHO-Ph-**	**>31.2**[d]	3.8 ± 0.3	>8.2	**0.08 ± 0.02**	**>390**	**3.9**
11	4-OH-Ph-	>12.5[d]	3.0 ± 0.8	>4.2	0.41 ± 0.08	>30.5	3.8
12	**4-CH_2OH-Ph-**	**13.1 ± 6.0**	1.5 ± 0.4	8.7	**0.09 ± 0.03**	**145.6**	**3.4**
13	**3-CH_2OH-Ph-**	**>25**[d]	**1.4 ± 0.2**	**>17.9**	**0.15 ± 0.03**	**>166.7**	**3.4**
14	**2-CH_2OH-Ph-**	**88 ± 32.0**	>10[e]	<8.8	**0.16 ± 0.03**	**550**	**3.4**
15	**4-F-Ph-**	>15.6[d]	**1.3 ± 0.2**	**>12**	0.31 ± 0.2	>50.3	4.3
16	3-F-Ph-	>12.5[d]	1.7 ± 0.5	>7.4	0.2 ± 0.1	>62.5	4.3
17	2-F-Ph-	>3.9[d]	–	–	–	–	4.3
18	2,4-F-Ph-	>7.8[d]	–	–	–	–	4.4
19	4-CF_3-Ph-	>3.9[d]	–	–	–	–	5.0
20	**3-CF_3-Ph-**	**>12.5**[d]	**1.1 ± 0.3**	**>11.4**	**0.04 ± 0.01**	**>312.5**	**5.0**
21	**2-CF_3-Ph-**	**22.7 ± 3.9**	**1.6 ± 0.4**	**14.2**	**0.07 ± 0.02**	**324.3**	**5.0**
22	**Pyridin-3-yl-**	**>31.3**[d]	**2 ± 0.6**	**>15.7**	**0.23 ± 0.01**	**>136.1**	**2.9**
23	**Pyridin-4-yl-**	**>50**[d]	**3 ± 0.8**	**>16.7**	**0.25 ± 0.01**	**>200**	**2.9**
24	Thiophen-2-yl-	>3.9[d]	–	–	–	–	3.9
25	Furan-2-yl-	>3.9[d]	–	–	–	–	3.2
Initial hit molecule		>31[d]	4.4 ± 0.8	>7.1	2.9 ± 0.5	>10.7	3.4
Doxorubicin[a]		0.2 ± 0.02	–	–	–	–	
Amphotericin B[b]		8.8 ± 0.3	0.06 ± 0.001	146.7	–	–	
Miltefosine[b]		85 ± 8.8	0.8 ± 0.2	106.3	–	–	
Fexinidazole[b,c]		>200[e]	3.4 ± 0.8	>58.8	0.6 ± 0.2	>333	

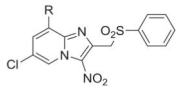

Compd	R-	CC_{50} HepG2 (μM)	IC_{50} *L. infantum* axenic amastigotes (μM)	*Selectivity Index (SI) Leishmania*[f]	IC_{50} *T. brucei brucei* trypomastigotes (μM)	*Selectivity Index (SI) Trypanosoma*[g]	cLogP[h]
Suramin[c]		>100[e]	–	–	0.03 ± 0.009	>3333	
Eflornithine[c]		>100[e]	–	–	13.3 ± 2.1	>7.5	

Best results are indicated in bold.

[a] Doxorubicin was used as a cytotoxic reference drug.

[b] Amphotericin B, Miltefosine and Fexinidazole were used as antileishmanial reference drugs.

[c] Fexinidazole, Suramin and Eflornithine were used as antitrypanosomal reference drugs.

[d] The product could not be tested at higher concentrations in aqueous medium.

[e] The CC_{50} or IC_{50} value was not reached at the highest tested concentration.

[f] SI = CC_{50} HepG2/IC_{50} *L. infantum*.

[g] SI = CC_{50} HepG2/IC_{50} *T. brucei brucei*.

[h] Weighted LogP were computed with MARVIN® software (ChemAxon).

Europe PMC Funders Author Manuscripts

Table 3

In vitro antileishmanial profile of hit compounds 13 and 23.

N°	Structure	IC_{50} *L. donovani* promastigotes (μM) & SI_{HepG2}	IC_{50} *L. donovani* intramacrophage amastigotes (μM) & SI_{HepG2}	IC_{50} *L. infantum* axenic amastigotes (μM) & SI_{HepG2}	CC_{50} HepG2 (μM)	CC_{50} THP1 (μM)
13	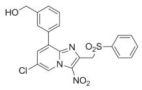	1.3 ± 0.2 *>19.2*	>10[d] -	1.4 ± 0.2 *>17.9*	>25[c]	>15[c]
23	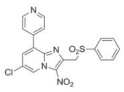	1.2 ± 0.4 *>41.7*	2.3 ± 0.6 *>21.7*	3.0 ± 0.8 *>16.7*	>50[c]	>25[c]
Initial Hit	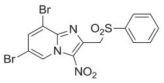	1.8 ± 0.8 *>17.2*	5.5 ± 0.2 *>5.6*	4.4 ± 0.8 *>7.0*	>31[c]	>25[c]
Doxorubicin[a]		–	–	–	0.2 ± 0.02	1.4 ± 0.5
Fexinidazole[b]		1.2 ± 0.2 *>166.7*	>50[d] –	3.4 ± 0.8 *>58.8*	>200[d]	>62.5[c]
Miltefosine[b]		3.1 ± 0.2 *27.4*	4.3 ± 1.7 *19.8*	0.8 ± 0.2 *106.3*	85 ± 8.8	>40[d]
Amphotericin B[b]		0.07 ± 0.01 *125.7*	0.4 ± 0.01 *22*	0.06 ± 0.001 *146.7*	8.8	3.6 ± 0.7

[a]Doxorubicin was used as a cytotoxic reference drug.

[b]Amphotericin B, Miltefosine and Fexinidazole were used as antileishmanial reference drugs.

[c]The product could not be tested at higher concentrations in aqueous medium.

[d]The CC_{50} or IC_{50} value was not reached at the highest tested concentration.

Europe PMC Funders Author Manuscripts

Table 4

8-Aryl-3-nitroimidazo[1,2-*a*]pyridines are bioactivated by kinetoplastid type 1 nitroreductases (NTR1).

	***L. donovani* promastigotes IC_{50} (μM)**		
	Wild-type	**$NTR1^{OE}$**	**$NTR2^{OE}$**
13	1.4 ± 0.07	0.07 ± 0.003	1.9 ± 0.04
23	1.5 ± 0.05	0.04 ± 0.009	2.0 ± 0.2
Initial hit molecule	1.9 ± 0.08	0.07 ± 0.002	3.0 ± 0.08
	***T. brucei brucei* trypomastigotes IC_{50} (μM)**		
	Wild-type		**$NTR1^{OE}$**
14	0.39 ± 0.07		0.19 ± 0.019
20	0.09 ± 0.002		0.04 ± 0.001
Nifurtimox	1.87 ± 0.05		0.6 ± 0.05

Europe PMC Funders Author Manuscripts

Table 5

Reduction potential modulation in the studied series.

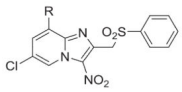

Compd	R-	E° (V)
4		−0.65
5		−0.69
13		−0.70
14		−0.70
20		−0.67
23		−0.64
Initial Hit 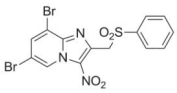		−0.59
Fexinidazole		−0.83

Cyclic voltammetry conditions: DMSO/TBAPF6, SCE/GC, 1 electron reversible reduction, values are given in volt and are corrected toward NHE.